Received: 30 November 2022 | Revised: 1 February 2023 | Accepted: 18 March 2023

DOI: 10.1002/smm2.1211

REVIEW

SmartMat Open Access WILEY

Advanced nanoengineering strategies endow high-performance layered transition-metal oxide cathodes for sodium-ion batteries

Jun Xiao[1,2] | Yang Xiao[1] | Jiayi Li[1] | Cheng Gong[1] | Xinming Nie[3] | Hong Gao[1,2] | Bing Sun[2] | Hao Liu[1,2] | Guoxiu Wang[2]

[1]Joint International Laboratory on Environmental and Energy Frontier Materials, School of Environmental and Chemical Engineering, Shanghai University, Shanghai, China

[2]Centre for Clean Energy Technology, School of Mathematical and Physical Sciences, Faculty of Science, University of Technology Sydney, Broadway, Sydney, New South Wales, Australia

[3]School of Physics and Electronic Engineering, Jiangsu Normal University, Xuzhou, Jiangsu, China

Correspondence

Xinming Nie, School of Physics and Electronic Engineering, Jiangsu Normal University, Xuzhou, Jiangsu 221116, China.
Email: nxinming@jsnu.edu.cn

Hao Liu, Joint International Laboratory on Environmental and Energy Frontier Materials, School of Environmental and Chemical Engineering, Shanghai University, Shanghai, China.
Email: hao.liu@uts.edu.au

Guoxiu Wang, Centre for Clean Energy Technology, Faculty of Science, University of Technology Sydney, Broadway, Sydney, NSW 2007, Australia.
Email: Guoxiu.Wang@uts.edu.au

Funding information

Australian Research Council, Grant/Award Numbers: DP180102297, FT180100705

Abstract

Considering the abundance and low price of sodium, sodium-ion batteries (SIBs) have shown great potential as an alternative to existing lithium-based batteries in large-scale energy storage systems, including electric automobiles and smart grids. Cathode materials, which largely decide the cost and the electrochemical performance of the full SIBs, have been extensively studied. Among the reported cathodes, layered transition-metal oxides (LTMOs) are regarded as the most extremely promising candidates for the commercial application of the SIBs owing to their high specific capacity, superior redox potential, and suitable scalable preparation. Nevertheless, irreversible structural evolution, sluggish kinetics, and water sensitivity are still the critical bottlenecks for their practical utilization. Nanoengineering may offer an opportunity to address the above issues by increasing reactivity, shortening diffusion pathways, and strengthening structural stability. Herein, a comprehensive summary of the modification strategies for LTMOs is presented, emphasizing optimizing the structure, restraining detrimental phase transition, and promoting diffusion kinetics. This review intends to facilitate an in-depth understanding of structure–composition–property correlation and offer guidance to the further development of the LTMO cathodes for next-generation energy storage systems.

KEYWORDS

cathode materials, layered transition-metal oxides, modification strategies, sodium-ion batteries

1 | INTRODUCTION

The ever-increasing demand for energy has greatly accelerated the consumption of traditional fossil fuels (coal, petroleum, and natural gas), which, in recent years, has resulted in energy crises and significant environmental pollution. The use of sustainable green resources, such as wind, solar, tide, and so forth, is the main choice for alleviating the aforementioned issues.[1–4] However, these green renewable resources are commonly intermittent and geographically distributed, which are hard to provide stable energy output for our daily life and production. Therefore, compact and fast-responding energy storage systems are necessarily explored for the storage and release of the energy produced by green resources.[5,6] Among diverse reported technologies, stationary secondary batteries have been considered one of the most promising solutions for this issue due to their high safety, low cost, environmental friendliness, and so on.[7,8] Particularly, lithium-ion batteries (LIBs) have made tremendous research progress and taken a large market share in the field of electronic products (electrical vehicles, portable electronic devices, etc.) during the past decades.[9–11] Unfortunately, low reserves and the uneven distribution of lithium in nature raise concerns about the price and availability of LIBs for grid-scale energy storage systems. Compared with lithium, sodium, which belongs to the same alkali metal series and shows analogous chemical properties, is earth-abundant and extensively distributed, subsequently giving rise to the low price of sodium-containing raw materials.[2] Moreover, many preceding studies have suggested that sodium-ion batteries (SIBs) behave with a similar working principle to LIBs.[3,6] Therefore, SIBs have attracted a great deal of attention from researchers and are considered one of the most potential substitutions for LIBs.[12–17]

Early research on SIBs can be dated back to almost the same period as LIBs, but the pursuit of LIBs with high energy density brings about the negligence for SIBs and impedes their further development. Nevertheless, the deficiency of lithium resources and its rising prices have set off the renaissance of SIBs in recent years.[18–20] Meanwhile, some techniques and knowledge obtained from the successful commercial application experience of LIBs can be directly adapted to SIBs on account of their similar properties, which tremendously expedites the rapid development of SIBs. Considering that cathode materials are the critical factor that affects the cost, cycling life, and energy density, considerable efforts have been made to develop cathode materials with fast kinetics, pre-eminent structural stability, and high specific capacity.[21–24] Up to now, various kinds of materials such as layered transition-metal oxides (LTMOs),[25–28] Prussian blue analogs,[29,30] polyanionic-type frameworks,[31,32] and organic substances,[33] have been extensively explored as positive electrodes for SIBs. Among these cathodes, LTMOs which can mainly be categorized into P2-, P3-, O2, and O3-type structures, have attracted extensive attention owing to their eminent merits such as high operating voltage, high specific capacity, facile synthesis, and so forth.[34–36] To be more specific, P or O represents the prismatic or octahedral coordination environment of Na, while the number reveals the oxygen packing sequence. P-type cathodes can provide direct and wide diffusion pathways for Na^+, realizing better rate performance and cycling life. O-type structures possessing high Na contents behave at high capacity and undergo complex phase revolutions during the sodiation/desodiation process.[15,19,28] Though some improvements have been achieved, there are still some weaknesses that impede their development to fulfill practical application requirements: (i) When used in SIBs, due to the higher weight, low standard potential, and larger ion radius of sodium, LTMO cathodes show lower energy density and slower kinetics than their counterparts in Li-ion batteries.[37–40] (ii) The structural rearrangement and revolution caused by Na^+ de/intercalation trigger large crystal parameter change and irreversible phase transition, which further lead to the collapse of the host structure and insufficient electrochemical performance.[41–44] (iii) This kind of material is sensitive to air and water, which will produce an insulated inorganic layer composed of Na_2CO_3 and NaOH. In addition, the H_2O molecule can insert into the Na layer or interchange the Na^+ with H^+, forming an adverse hydration phase.[45,46] All these parasite reactions bring about an inhibited ability for Na^+ insertion/extraction and unfavorable electrochemical performance. Nanoengineering, which endows electrode materials with numerous advantages, including short diffusion paths, improved structural stability, enhanced reactivity, small polarization, and so on, is beneficial to solve these above-mentioned problems and realize better cycle life and rate performance.[18,21] These phenomena suggest that it is significant to optimize the structure and composition of the LTMO electrode materials to achieve positive progress of the SIBs.

In this review, we comprehensively summarize the existing modification strategies to ameliorate the electrochemical performance of LTMO cathodes for SIBs, focusing primarily on ion substitution, coating technique, structure design, and mixed phases. The tactics described above are beneficial for enhanced structural stability, promoted fast kinetics, and restrained irreversible phase transition. In the meantime, the

relationship between the inner Na^+ storage mechanism and structural transformation behind the sodiation/desodiation process is discussed in detail to further clarify the strengths of various methods. At last, some perspectives for the future development of LTMO electrode materials for SIBs are also introduced. We expect that the insights in this review can expedite the progress toward the triumphant commercial application of SIBs.

2 | ELEMENT SUBSTITUTION

Element substitution, also known as element doping, is one of the most common ways to regulate the crystal structure of LTMO cathode materials and is feasible for mass production. This strategy means to supersede some of the composition elements in the original sample with a few other ions, which can be added during the preparation of the undoping electrode, contributing to enhanced rate performance, stable structure, high energy density, and so forth.[47,48] Element substitution is mainly subdivided into two categories: cationic and anionic substitution, according to the charge of the doping elements. Moreover, modulation of the microstructure with both kinds of ions to accommodate the volume change and optimize performance has also received much attention.

2.1 | Cation substitution

Cation substitution manifests doping some ions with a positive charge (Li^+, Mg^{2+}, Zn^{2+}, Al^{3+}, etc.) into the transition-metal (TM) site or Na^+ site.[1,35,42] The properties of ultimate samples adjusted at the nanoscale may vary from the amount and types of the elements, which suggests the adjustability of this approach. And different elements may provoke synergistic effects when doped into the host structure at the same time. This strategy manifests diverse strengths as follows: First, it can inhibit the glide of the TM layers, restrain the adverse phase transition, and suppress the Jahn–Teller effect of the TM ions.[49–52] Second, doping ions in TM layers with high redox couple can enhance the voltage platform, and some can even induce the reversible oxygen redox activity benefiting from the strong TM 3d (4d)-O 2p covalency and unhybridized O 2p orbitals, leading to extra specific capacity and enhanced energy density which is essential for practical utilization.[53–55] Then, LTMO cathodes with optimized composition may protect the material from erosion caused by water or air, greatly reducing the cost of storage and transportation.[56] Finally, unusual site-selective substitution in the Na site serves as a pillar to stabilize the structure by increasing electrostatic cohesion between neighboring TMO_2 layers, inducing a pinning effect to achieve a zero-strain layered cathode, reducing the activation energy to improve diffusion kinetics, thus realizing enhanced rate performance.[57,58]

Na^+/vacancy ordering induced by ionic radii and Fermi level of TM occurred when Na^+ was extracted from the host structure leads to fast capacity decay and slow Na^+ mobility. Moreover, irreversible phase transitions caused by layer gliding after Na^+ extraction during the charge process give rise to large voltage hysteresis and large volume changes.[2,8,52] Jin et al. prepared a new high Na content P2-type cathode $Na_{0.85}Li_{0.12}Ni_{0.22}Mn_{0.66}O_2$ through a facile solid-state reaction by introducing Li into the Ni site, effectively suppressing the irreversible P2–O2 phase transition, which generates large volume change (23%) and mitigates Na^+/vacancy ordering as well as charge ordering.[59] Thus, the as-prepared positive material demonstrates a solid–solution reaction mechanism when deeply charged, confirmed by the in-situ X-ray diffraction (XRD) measurement (Figure 1A). And it achieves excellent rate performance and outstanding cycle stability simultaneously. Xu and coworkers reported an interesting Ti-substituted electrode material $Na_{0.67}[Li_{0.21}Mn_{0.59}Ti_{0.2}]O_2$, which can show a high reversible capacity up to 231 mA h/g caused by the synergistic redox reaction of manganese and oxygen when cycled at 0.2 C.[60] Moreover, benefiting from the reduced repulsion between adjacent TM layers and suppressed irreversible manganese migration caused by additional oxygen redox, this material maintains its P2-type structure during the whole process with an extremely small volume strain (0.7%) with almost no change in parameter c during the charging process, which is much smaller than the variation of c-axis in $NaMnO_2$ when changed into $Na_{0.70}MnO_2$ (5.807–16.737 Å) (Figure 1B).[27,60] Zhou's group introduced three cationic ions (e.g., Ni^{2+}, Cu^{2+}, and Mg^{2+}) into the Na_xMnO_2 host structure to replace part Mn and the prepared $Na_{0.8}Mn_{0.6}Ni_{0.2}Cu_{0.1}Mg_{0.1}O_2$ (NaMNCuMg) electrode material.[61] The obtained cathode can maintain 82.9% of its initial specific capacity after 500 cycles at a high rate of 500 mA/g because doping postpones the adverse P2–O2 phase to a high voltage range. In addition, divalent cation doping increases the average oxidation state of Mn, thereby eliminating the Jahn–Teller effect of Mn^{3+}. Meanwhile, Cu doping endows this material with excellent air/water stability, confirmed by the aging test (Figure 1C).

As illustrated by the calculated ion-removing energies, Shen et al. found that Ca^{2+} is inclined to dope into the Na^+ site, which can act as a "pillar" to stabilize the

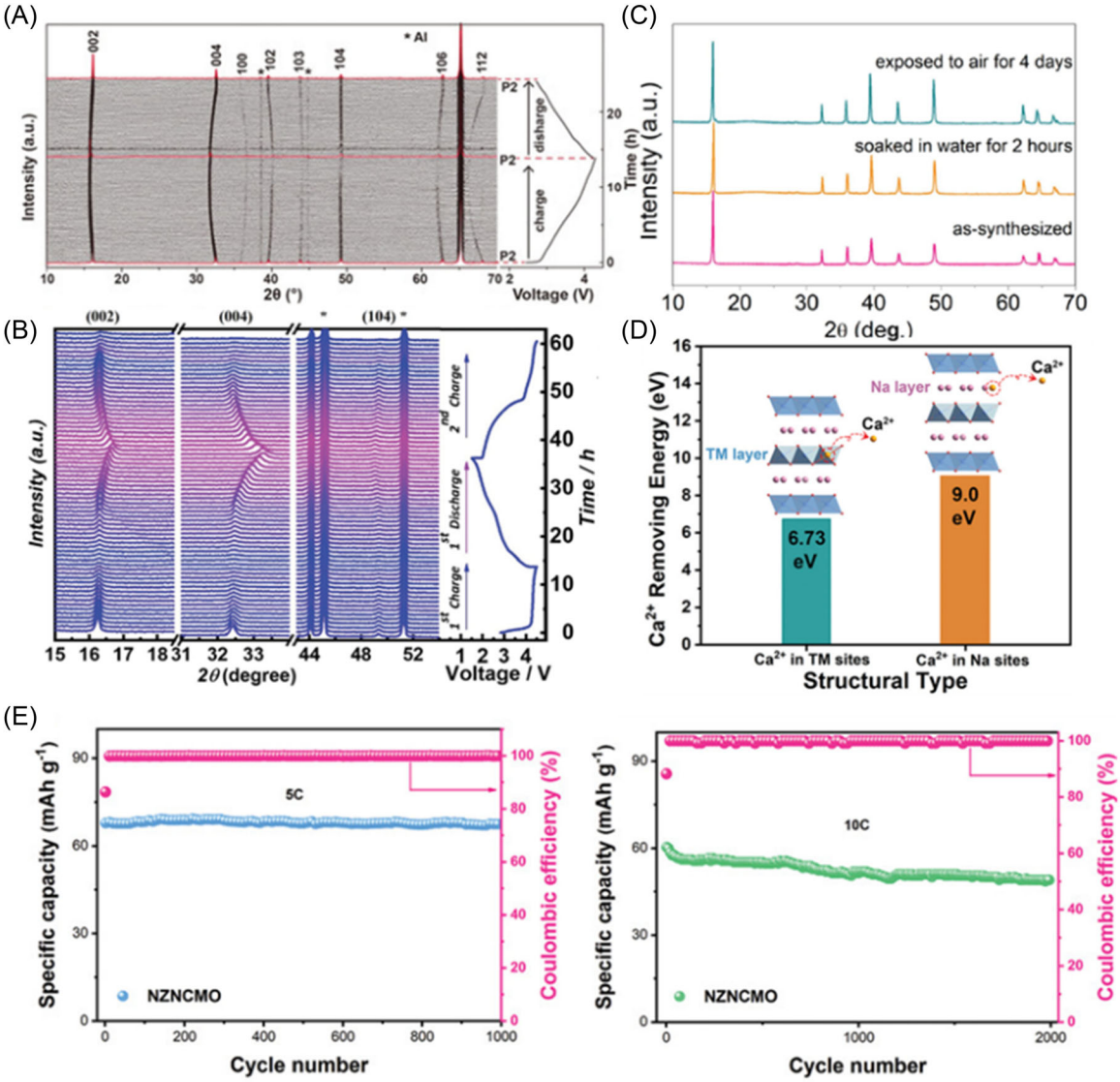

FIGURE 1 (A) In situ X-ray diffraction (XRD) patterns collected during the first charge/discharge of the P2–NLNMO electrode tested at 0.1 C in a voltage window of 2.0 and 4.3 V. Reproduced with permission: Copyright 2020, Wiley-VCH.[59] (B) In situ XRD patterns of $Na_{0.67}[Li_{0.21}Mn_{0.59}Ti_{0.2}]O_2$ collected during the first cycle and the second charge. The inset star symbols represent the peak of Al. Reproduced with permission: Copyright 2020, Wiley-VCH.[60] (C) XRD patterns of P2–NaMNCuMg. Reproduced with permission: Copyright 2020, Elsevier B.V.[61] (D) Two Ca-doped crystal structure models with the corresponding Ca^{2+} removing energies. Reproduced with permission: Copyright 2021, Wiley-VCH.[62] (E) Long-term cycling performance of NZNCMO at relatively high rates of 5 and 10 C. Reproduced with permission: Copyright 2021, Wiley-VCH.[63]

crystal structure (Figure 1D).[62] More specifically, this pillar effect directly refrains from the detrimental Na^+/vacancy ordering to ensure enhanced Na^+ diffusion kinetics and inhibits the gliding of TM layers at a deep desodiation state to avoid P2–O2 phase transition. Compared with Na–O bonds, the bonding energy of the Ca–O bond becomes higher on account of the highly valent and small radius of Ca^{2+}. As a result, the stable configuration enables reversible anionic redox activities. Peng and co-workers prepared a co-substituted $[Na_{0.67}Zn_{0.05}]Ni_{0.18}Cu_{0.1}Mn_{0.67}O_2$ cathode in which Zn and Cu occupy Na and TM sites of the original material, respectively.[63] The Cu^{2+} doping can stabilize the metal layers, while the O^{2-}–Zn^{2+}–O^{2-} "pillar" with strong electrostatic cohesion mitigates crack formation and facilitates interfacial diffusion kinetics. Therefore, this electrode achieves pre-eminent long-cycle stability at high current density (Figure 1E). Chen et al. modified the representative P2–$Na_{2/3}Ni_{1/3}Mn_{2/3}O_2$ cathode with Li, Mg, and Ti, which can achieve high theoretical capacity, strengthen structural stability, and promote high redox potential, respectively.[64] Moreover, Li substitution

increases the Na^+ content and changes local structure, contributing to increased TM layers gliding energy barriers. Therefore, the as-prepared material shows excellent cycling life.[64] More interestingly, introducing more cation ions even contributes to generating high entropy materials, which represent multicomponent elements co-existing in a single phase without the formation of other impurities, as compared to ordinary metal oxide systems with limited elements. This kind of high entropy material shows eminent structural robustness, greatly ameliorating the cycling performance of LTMO cathode.[65,66]

2.2 | Anion substitution

Partial cationic substitution has been proven to be a useful way to enhance the overall electrochemical performance of LTMO cathodes. However, most of these selected doping elements are electrochemically inactive, so that the improved cycling life is brought at the expense of some specific capacity owing to reduced redox center.[26] Reported results show that anionic substitution (F^-) in the oxygen site is also a valid measure to ameliorate the structural stability and increase the specific capacity because the strong electronegativity of F^- strengthens the chemical bonds and less negative charge decreases the TM valence. In addition, F-substitution is conducive to suppressing the dissolution of TM ions into the electrolyte, accelerating the Na^+ diffusion rate, mitigating voltage decaying, and destroying the cation ordering.[67–69] Kang et al. prepared a series of F-doping samples $Na_{0.6}Mn_{0.7}Ni_{0.3}O_{2-x}F_x$ ($x = 0$, 0.03, 0.05, and 0.07) and found that the modified electrodes retain the original P2 structure but with changed crystal parameter (Figure 2A).[70] Apparently, the left shift of (002) peaks indicates the enlarged adjacent layer distance along *c*-axis, which is in favor of accelerated reaction kinetics. Moreover, the blue shift of E_g and A_{1g} bands in Raman spectra proves that F^- ions replace partial oxygen, leading to shorter TM–O bond lengths. Through evaluating the specific capacities, cycling performance, and rate capability, the optimal value is F-0.05. Liu and coworkers proposed that F^- substitution alters local interatomic distance and is prone to reduce the valence of Mn ions from +4 to +3 rather than having an effect on the oxidation state of Ni ions in the $Na_{2/3}Ni_{1/3}Mn_{2/3}O_{1.95}F_{0.05}$ cathode, confirmed by the X-ray absorption near edge structure (XANES) (Figure 2B).[71] Redistribution of Mn/Ni and ordering disruption of Na^+ induced by F doping stabilizes the phase structure so that this cathode delivers distinguished capacity retention over 2000 cycles at 55°C (75.6% at 10 C). This means this battery system can behave with improved output power because the increased temperature contributes to accelerated reaction kinetics.

2.3 | Anion/cation dual-substitution

In addition to single cationic or anionic ion doping, dual-substitution with both of them has been considered a useful method to ameliorate the performance of LTMO cathodes, which can combine the positive effect of cations and anions as mentioned above.[74,75] For instance, Chae et al. doped Al and F into tunnel-type $Na_{0.44}MnO_2$ (NMO), successfully preparing a new layered structure with 2D diffusion pathways.[72] The homogeneous distribution of Al/Mn and F/O without ordering is confirmed by Fourier synthesis maps, which also clearly point out the two types of Na^+ (Figure 2C). Compared to the original sample, the as-synthesized $Na_{0.46}Mn_{0.93}Al_{0.07}O_{1.79}F_{0.21}$ (AFNMO) electrode shows improved rate performance (125.5 mA h/g at 5 C) and capacity retention (89.1% over 500 cycles). From the bond valence energy landscape (BVEL) calculations and ex situ XRD measurements, this codoping material shows lower diffusion energy barriers, restrained volume change, and mitigated Jahn–Teller effect of Mn^{3+}, thereby realizing high electrochemical performance. Cui and coworkers proposed a significant ex situ F and in situ Mg dual-substitution tactic to prepare the $Na_{0.524}Mg_{0.146}Ni_{0.15}Fe_{0.20}Mn_{0.65}F_{0.05}O_{1.95}$ (NM–NFMF005) cathode in which Mg^{2+} ions were introduced into the Na sites by a simple electrochemical method.[73] Moreover, F doping further shortens the interatomic bond length and enlarges the *d*-spacing for Na^+ diffusion. Therefore, this dual-site doped electrode shows a reinforced structure, enhanced electrochemical performance, and a solid–solution reaction mechanism without the emergence of a new phase (Figure 2D).

3 | COATING TECHNIQUE

Some reports have found that LTMO cathode materials are prone to react with electrolytes during the sodiation/de-sodiation process.[6,14,16,22,39] These parasite reactions would exfoliate the active materials from the current collector, produce thick and uneven insulating cathode-electrolyte interface layers (Na_2CO_3), and cause harmful phase transition.[46,54] In addition, the generated HF product from the degradation of the component ($NaPF_6$) in the electrolyte further attacks the inner active material and consumes more Na^+, bringing about fast capacity attenuation. To resolve these issues, researchers explored coating

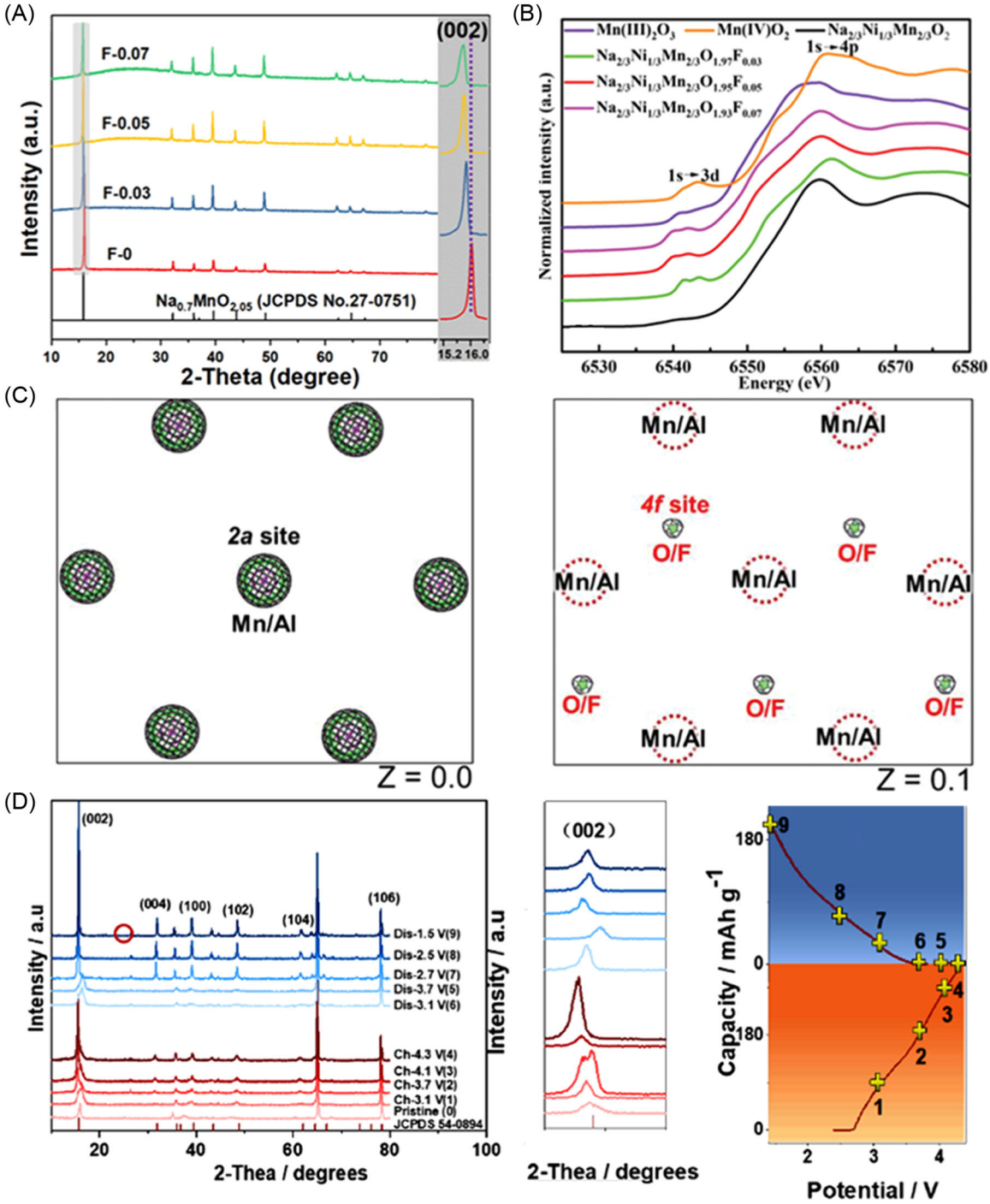

FIGURE 2 (A) X-ray diffraction (XRD) patterns for F-0, F-0.03, F-0.05, and F-0.07 and the corresponding magnified (002) peaks. Reproduced with permission: Copyright 2021, American Chemical Society.[70] (B) Mn K-edge XANES spectra of different samples. Reproduced with permission: Copyright 2020, WILEY-VCH.[71] (C) Fourier maps for the transition-metal layer and oxygen and fluorine layer. Reproduced with permission: Copyright 2020, WILEY-VCH.[72] (D) The ex situ XRD patterns of P2-type NM–NFMF005. Reproduced with permission: Copyright 2021, Elsevier B.V.[73]

strategy as another valid way to modify LTMO cathode materials. These protective nanolayers on the cathode surface can prevent active materials from direct contact with electrolytes, thus inhibiting harmful side reactions.[76,77] On the other hand, they can also minimize large volume change, mitigate irrevocable phase transition, and restrain metal dissolution. In the meantime, these coating layers are prioritized for the materials with good conductivity so that they decrease the interface resistance of LTMO cathodes

and enhance the rate performance and cycling stability, and some can even increase the specific capacity.[78,79]

3.1 | Metal phosphate coating

Metal phosphate coating is one of the most common ways to modify LTMO cathodes with protective layers to improve the overall performance, which can be prepared by facial sol–gel, melt-impregnation, and chemical coprecipitation methods. To be more specific, the high electronegativity of the anionic phosphate groups is beneficial for increasing the resistance to prevent active materials from reacting with electrolytes.[76] Besides, $NaTi_2(PO_4)_3$ (NTP) coating material with NASICON-type structure belonging to the phosphate family is composed of corner-shared TiO_6 and PO_4 polyhedrons, and it shows robust structure and provides fast diffusion pathways for Na^+ during the intercalation/deintercalation process owing to the three-dimensional crystal framework. And TM ions with high valence can dope into the crystal structure to change the parameter, such as increasing the layer spacing, further accelerating the diffusion kinetics.[80–84]

Jo et al. adopted a bioinspired β-$NaCaPO_4$ nanolayer (5–10 nm) on the surface of the popular P2-$Na_{2/3}[Ni_{1/3}Mn_{2/3}]O_2$ cathode via a high-temperature calcination reaction between Ca–P–O-based compound and residual sodium residues (Na_2CO_3 and NaOH).[81] Due to the strong bonding among Ca^{2+} and PO_4^- ions, this eco-friendly and nontoxic protective layer shows excellent chemical and thermal stability. The coating layer can effectively clear away HF and H_2O, originating from the decomposition of the electrolyte component. Therefore, the coated sample not only suggests prolonged cycling life (Figure 3A), but also displays stable thermal properties in contrast to the bare material verified by thermogravimetry (TG) and differential scanning calorimetry tests (Figure 3B). The same group also reported another $NaPO_3$ coating material synthesized by the melt-impregnation method at 300°C using the $NH_4H_2PO_4$ and sodium-containing byproducts as reactants to stabilize the surface (Figure 3C).[82] It plays a similar role to β-$NaCaPO_4$ mentioned above. And benefiting from the good effect of the $NaPO_3$ nanolayer with a thickness of 10 nm on the electrode surface, the obtained composite material can maintain 73% of its initial specific capacity after 300 cycles when assembled in full batteries with hard carbon as the anode. Moreover, this coating material successfully inhibits oxygen release at a deep charge state because it can postpone the formation of manganic–manganous oxide. Another interesting NTP material with a NASICON-type structure has been extensively studied as a coating layer to optimize the performance of LTMO cathodes due to its special open structural framework.[83,84] In 2020, Li and coworkers successfully introduced the NTP protective layer on the surface of $Na_{0.67}Co_{0.2}Mn_{0.8}O_2$ (NCM) cathode by a simple wet chemical method and as confirmed by the transmission electron microscope (TEM) measurement, the layer thickness is about 20 nm (Figure 3D).[85] The as-prepared NCM@NTP composite shows better cycling stability (capacity retention of 92.3% after 150 cycles), lower charge transfer resistance (26.4 Ω), and better rate performance (70.7 mA h/g at 20 C) than bare NCM. Deng et al. found that the NTP not only inhibited the irreversible P2–O2 phase transition that occurred in P2-type $Na_{0.65}[Mn_{0.70}Ni_{0.16}Co_{0.14}]O_2$ (NMNCO) but also enhanced the specific capacity.[86] Besides that, the Ti^{4+} with an ion radius (0.61 Å) smaller than Na^+ (1.02 Å) doped into the host structure decreases the thickness of TM layers while increasing the *d*-spacing for Na^+ diffusion, as verified by the shift of (002) peaks in the XRD patterns. What is more, the ameliorated diffusion kinetics was confirmed by the calculated activation barrier energy, further suggesting the merit of NTP modification (Figure 3E).

3.2 | Metal oxide coating

Apart from metal phosphates, metal oxide coating is also a good option to optimize the properties because they isolate the active material and electrolyte, thereby preventing the parasite reaction and dissolution of TM ions. This artificial solid electrolyte interphase (SEI) film mitigates volume change and enables stable structure.[87–89] The atomic layer deposition (ALD) technique has been widely used in the coating field for electrode materials owing to the merits, including controllable thickness and homogeneous coating layers, which is difficult to achieve by traditional methods as well as suitable for lots of different coating materials (TiO_2, SnO_2, and Al_2O_3).[90]

For instance, Hwang et al. coated nanosized Al_2O_3 on the surface of microspherical $Na[Ni_{0.6}Co_{0.2}Mn_{0.2}]O_2$ cathode through the facile dry-balling method (Figure 4A).[91] The densely covered Al_2O_3 scavenges the HF generated by the decomposition of $NaPF_6$ in the electrolyte and forms new stable AlF_3 material on the outmost edge of the Al_2O_3 protective layer, further protecting the active materials from HF attack. Thus, the modified composite shows excellent structural stability and maintains 75% of its initial specific capacity after 300 cycles in a pouch-type full cell. Kong's group reported

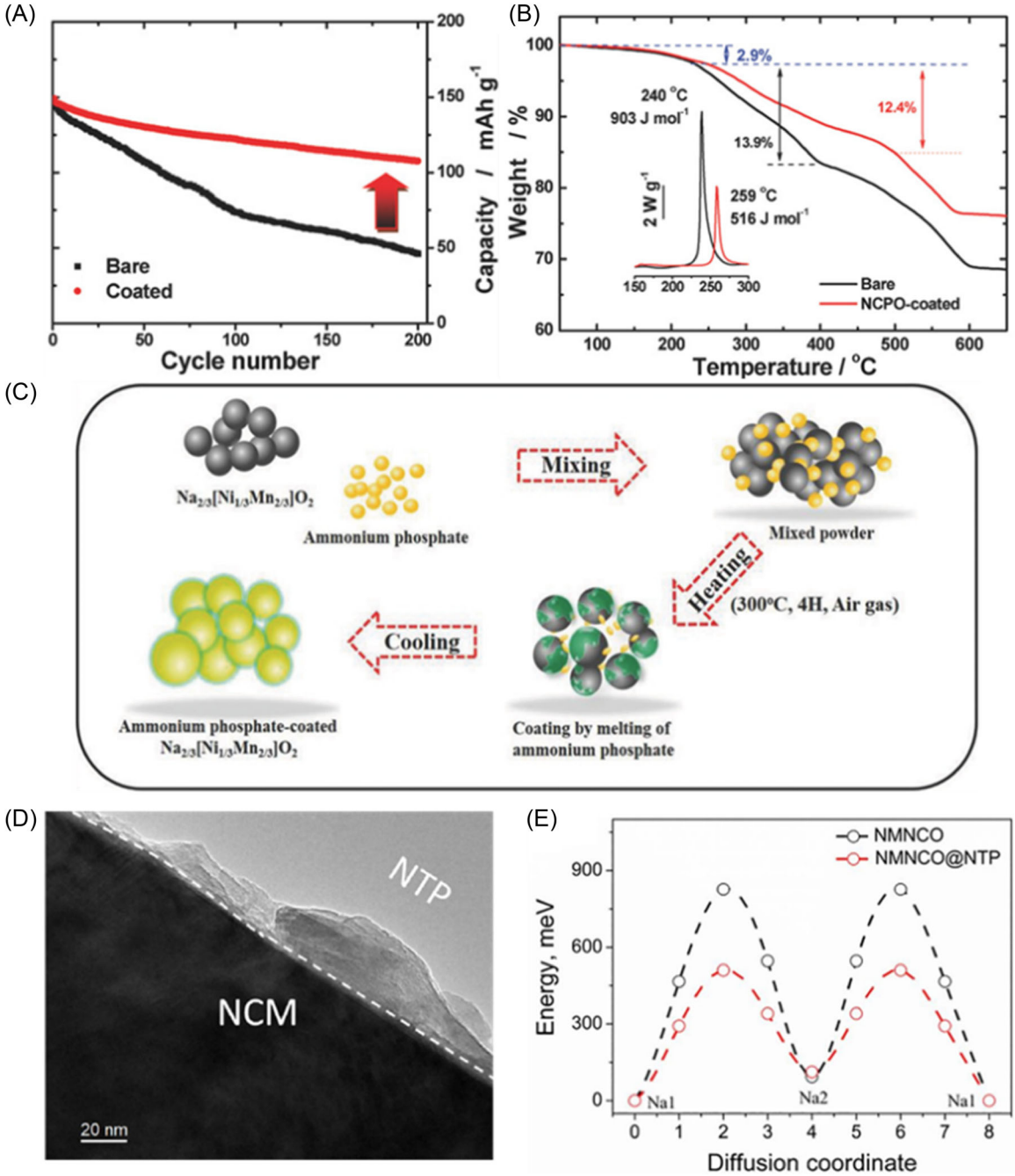

FIGURE 3 (A) Cycle life of bare and $NaCaPO_4$-coated $Na_{2/3}[Ni_{1/3}Mn_{2/3}]O_2$ during 200 cycles. (B) TG curves of 4.3 V charged bare and $NaCaPO_4$-coated $Na_{2/3}[Ni_{1/3}Mn_{2/3}]O_2$ powders (insert: corresponding differential scanning calorimetry [DSC] curves). Reproduced with permission: Copyright 2018, WILEY-VCH.[81] (C) Schematic illustration of melt-impregnation of $NaPO_3$ coating on $Na_{2/3}[Ni_{1/3}Mn_{2/3}]O_2$. Reproduced with permission: Copyright 2018, WILEY-VCH.[82] (D) Transmission electron microscopy (TEM) image of NCM@NTP. Reproduced with permission: Copyright 2020, Elsevier B.V.[85] (E) The activation barrier energy for Na^+ diffusion of pristine NMCNO and NMNCO@NTP materials. Reproduced with permission: Copyright 2020, Elsevier B.V.[86]

that a MgO coating layer (a mass ratio of 1.5%) with a thickness of 10 nm on $Na_{0.67}Mn_{0.5}Fe_{0.5}O_2$ (MF) surface not only suppresses parasite reactions but also enhances interface conductivity and e^-/Na^+ migration (Figure 4B).[92] Meanwhile, a small fraction of Mg doping decreases the migration energy barriers for Na^+ diffusion. Moreover, MgO coating inhibits the change of the crystal structure and irreversible P2–P′2 phase transition of MF by preventing TM ions from dissolution and reducing the change in interlay spacing (d), as confirmed by in situ XRD measurement (Figure 4C). Yu and coworkers coated the $NaMn_{0.33}Fe_{0.33}Ni_{0.33}O_2$ (MFN)

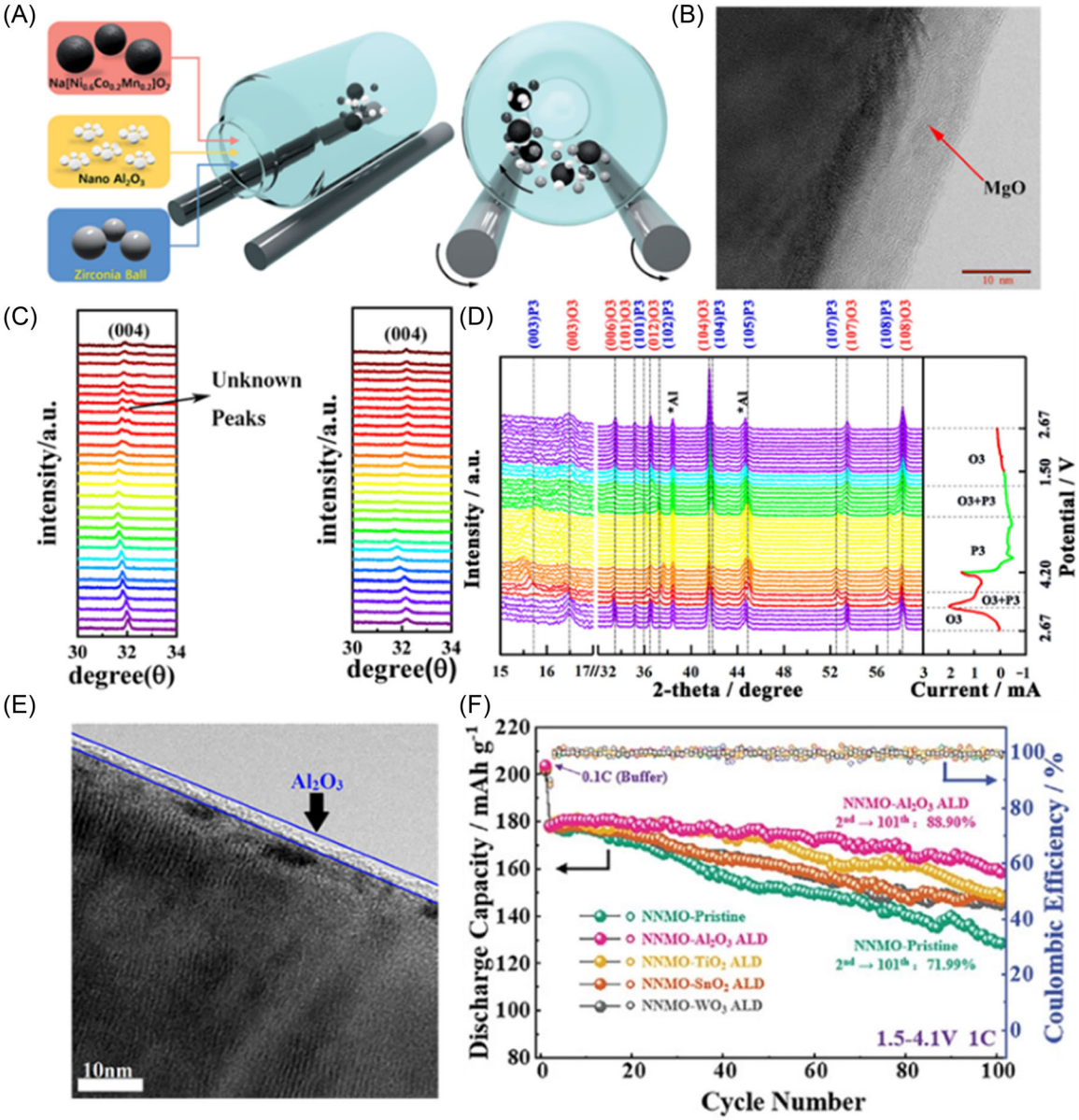

FIGURE 4 (A) Schematic illustration of the ball-mill coating process for fabricating an Al_2O_3-coated $Na[Ni_{0.6}Co_{0.2}Mn_{0.2}]O_2$ cathode. Reproduced with permission: Copyright 2017, The Royal Society of Chemistry.[91] (B) High-resolution transmission electron microscopy (HRTEM) image of MgO@MF. (C) The (004) peak of the MF and MgO@MF. Reproduced with permission: Copyright 2019, Elsevier B.V.[92] (D) In situ X-ray diffraction (XRD) patterns of TiO_2@MFN during the charge–discharge process. Reproduced with permission: Copyright 2020, American Chemical Society.[93] (E) TEM images of the uncycled Al_2O_3 atomic layer deposition (ALD)-coated $Na_{2/3}Ni_{1/3}Mn_{2/3}O_2$ composite electrode. Reproduced with permission: Copyright 2017, American Chemical Society.[94] (F) Cycling stabilities of five coated electrodes at 1 C. Reproduced with permission: Copyright 2021, WILEY-VCH.[95]

cathode with chemically stable TiO_2 via a simple solid-state reaction.[93] The TiO_2 coating accompanying partial Ti^{4+} doping effectively alleviates the Jahn–Teller effect of Mn^{3+} by decreasing its ratio and shrinking the TM–O and O–O bonds that are beneficial for the stable structure. Therefore, the as-prepared MFN@TiO_2 composite electrode achieves reversible phase transition (O3–P3) as compared to pristine MFN (Figure 4D). A homogeneous Al_2O_3 layer was introduced into $Na_{2/3}Ni_{1/3}Mn_{2/3}O_2$ by Alvarado et al. via the ALD technique (Figure 4E). This protective layer decreases inorganic species (carbonate) in the cathode electrolyte interphase (CEI) layer and reduces the resistance, thereby enhancing the Coulombic efficiency and mechanical stability.[94] Meanwhile, Ji et al. anchored different metal oxide nanolayers by using the ALD method to prevent deformation of the CEI layer on the $Na_{2/3}Ni_{1/3}Mn_{2/3}O_2$ (NNMO) surface and dissolution of TM ions, which

caused serious capacity degradation.[95] These protective layers effectively suppress the side reactions and contribute to the formation of a simple and stronger CEI layer, so modified samples show excellent cycling life (Figure 4F). More interestingly, the NNMO–Al_2O_3 ALD electrode shows better performance than other samples because of its highest formation energy of Mn vacancy.

3.3 | Metal fluoride coating

Except for the above-mentioned materials, metal fluorides, which were widely applied to modify cathode materials for LIBs, have attracted much attention as promising coating materials owing to their inert property and stable structure.[96] Sun et al. found that bare Na $[Ni_{0.65}Co_{0.08}Mn_{0.27}]O_2$ cathode showed numerous intraparticle cracks after cycling because the electrolyte eroded the material surface and further damaged the bulk structure, leading to the destruction of mechanical integrity and fast capacity loss. After coating AlF_3 via a simple dry ball-milling method, this stable, protective material successfully shields the cathode from electrolyte attack, thus inhibiting the infiltration of electrolyte into the bulk structure and realizing prolonged cycle stability.[96] Liu et al. discovered that AlF_3-coated $Na_{0.5}Ni_{0.25}Mn_{0.75}O_2$ (NNMO) cathode greatly alleviates the damage or pulverization of the bare NNMO structure ascribing to accumulated inner stress during repeated sodiation/desodiation process, which brings about the destruction of SEI layer and the exfoliation of active material (Figure 5A).[97]

3.4 | Carbon and polymer coating

Though these inorganic coating materials enhance cycle stability and inhibit the side reaction, their effects on improving the rate performance are not outstanding due to their relatively low conductivity. In contrast, conductive carbon coating materials with porous structures, which facilitate electron transfer, are conducive to rate performance amelioration other than stabilizing the crystal structure.[100,101] Uniform polydopamine-derived carbon coating layer synthesized via a conventional method was reported to improve the electrochemical properties of the P2-type $Na_{0.80}Ni_{0.22}Zn_{0.06}Mn_{0.66}O_2$ cathode (Figure 5B).[98] The carbon layer with a thickness of 5 nm restrains the Na^+ loss at the cathode surface, which is inclined to bring forth detrimental Na_2CO_3/NaOH during electrode fabrication. Compared with the original sample, the obtained composite electrode shows tremendously enhanced rate capacity (Figure 5C,D). Polymer coating is also a good choice not only due to its low-temperature synthesis but also for the mechanical flexibility different from other coating materials. Furthermore, it helps encapsulate cathode materials with consecutive ionic conductive coating layers. Some strong polar atoms or groups on the polymer materials even anchor TM ions on the surface of the active material to achieve a more stable interface nanolayer.[102,103] Lu et al. coated polypyrrole (PPy) on $Na_{0.7}MnO_{2.05}$ hollow microspheres (NMOHS) by a facile chemical ice water bath route (Figure 5E).[99] The hollow structure mitigates volume change and shortens the diffusion pathway for ion/electron, while the PPy coating layer ameliorates the conductivity, inhibits Mn ion dissolution, and stabilizes the structure. Therefore, the as-synthesized NMOHS@PPy composite cathode has better cycling life and rate performance than the pure electrode.

4 | STRUCTURE DESIGN

LTMO cathodes for SIBs always suffer from slower reaction kinetics and larger volume change than their counterparts used for LIBs due to the large size of Na^+. Rational morphology and structure design are conducive to shortening the diffusion pathways for Na^+, mitigating the mechanical stress caused by repeated Na^+ intercalation/deintercalation, and suppressing the irreversible phase transition to realize better rate capacity and cycle stability.[104,105] Furthermore, a special tightly stacked structure with high tap density is beneficial to improve the volumetric energy density, which is a key factor that influences the practical application of LTMO cathodes. A well-designed internal structure can even activate reversible anionic redox to get high specific capacity; therefore, the energy density is also enhanced.[106]

4.1 | Microsphere structure

Constructing microspherical LTMO cathodes with homogeneous size distribution helps build close-packed arrays to improve the tap density, which means that the space for batteries to be packed can be minimized when used in practical applications. In addition, the fluidity and dispersity of this structure enable the preparation of better electrodes.[107] Thus, this distinctive structure endowed with high volumetric energy density goes far toward achieving the commercial application of next-generation cathodes. Microspherical P2–$Na_{0.7}CoO_2$ (s–NCO) electrode prepared by facile self-templating method inherits the regular structure of the $CoCO_3$ precursors; compared with the irregular sample (i–NCO),

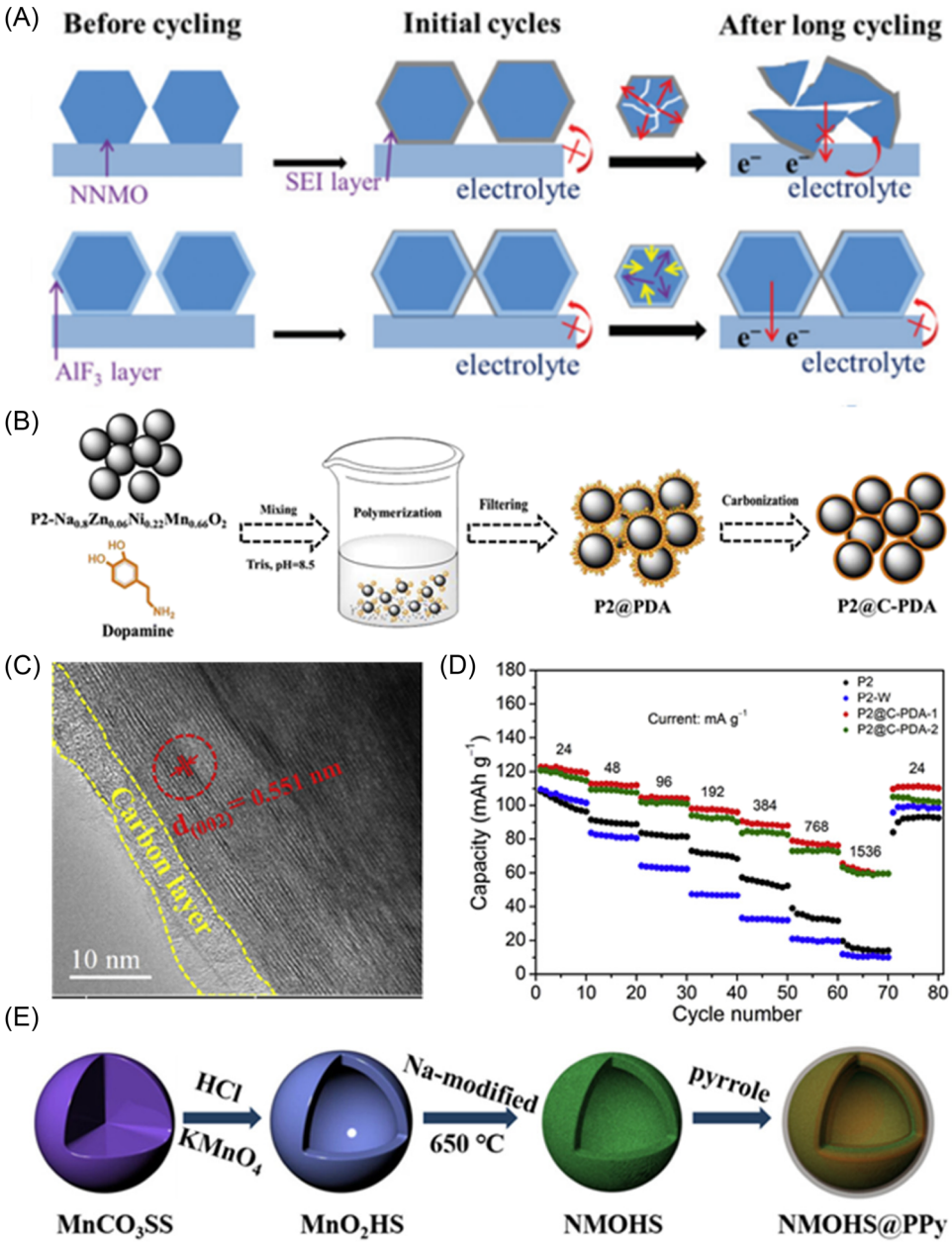

FIGURE 5 (A) Schematic of morphology–structure change in pristine AlF_3 coated and $Na_{2/3}Ni_{1/3}Mn_{2/3}O_2$ (NNMO) electrodes on electrochemical cycling. Reproduced with permission: Copyright 2018, The Royal Society of Chemistry.[97] (B) Schematic illustration of the preparation process of the P2@C–PDA sample. (C) High-resolution transmission electron microscopy (HRTEM) images of the carbon-coated samples. (D) Rate performance of the bare and carbon-coated samples. Reproduced with permission: Copyright 2019, Elsevier Ltd.[98] (E) Schematic illustration for fabrication of $Na_{0.7}MnO_{2.05}$ hollow microspheres (NMOHS) and NMOHS@PPy. Reproduced with permission: Copyright 2019, American Chemical Society.[99]

the s–NCO cathode suggests greatly enhanced cycle life (Figure 6A,B).[108] This may be ascribed to the regular structure with high crystallinity, which worked as an effective cushion against volume stress originating from repeated sodiation/desodiation process. Meanwhile, its special morphology effectively reduces the contact area between the active material and the electrolyte to mitigate harmful side reactions and dissolution of TM ions, while primary nanoparticles shorten the diffusion pathways to enhance rate performance.[108] Urea-assisted hydrothermal reaction is a facile and effective way to prepare a microsphere structure composed of nanoparticles by comparison with the coprecipitation method, which demands concise control of the pH, stir speed, and other reaction parameters. The $Na_{0.66}(Ni_{0.13}Mn_{0.54}Co_{0.13})O_2$ (Na-NMC-180) buckyballs cathode synthesized at

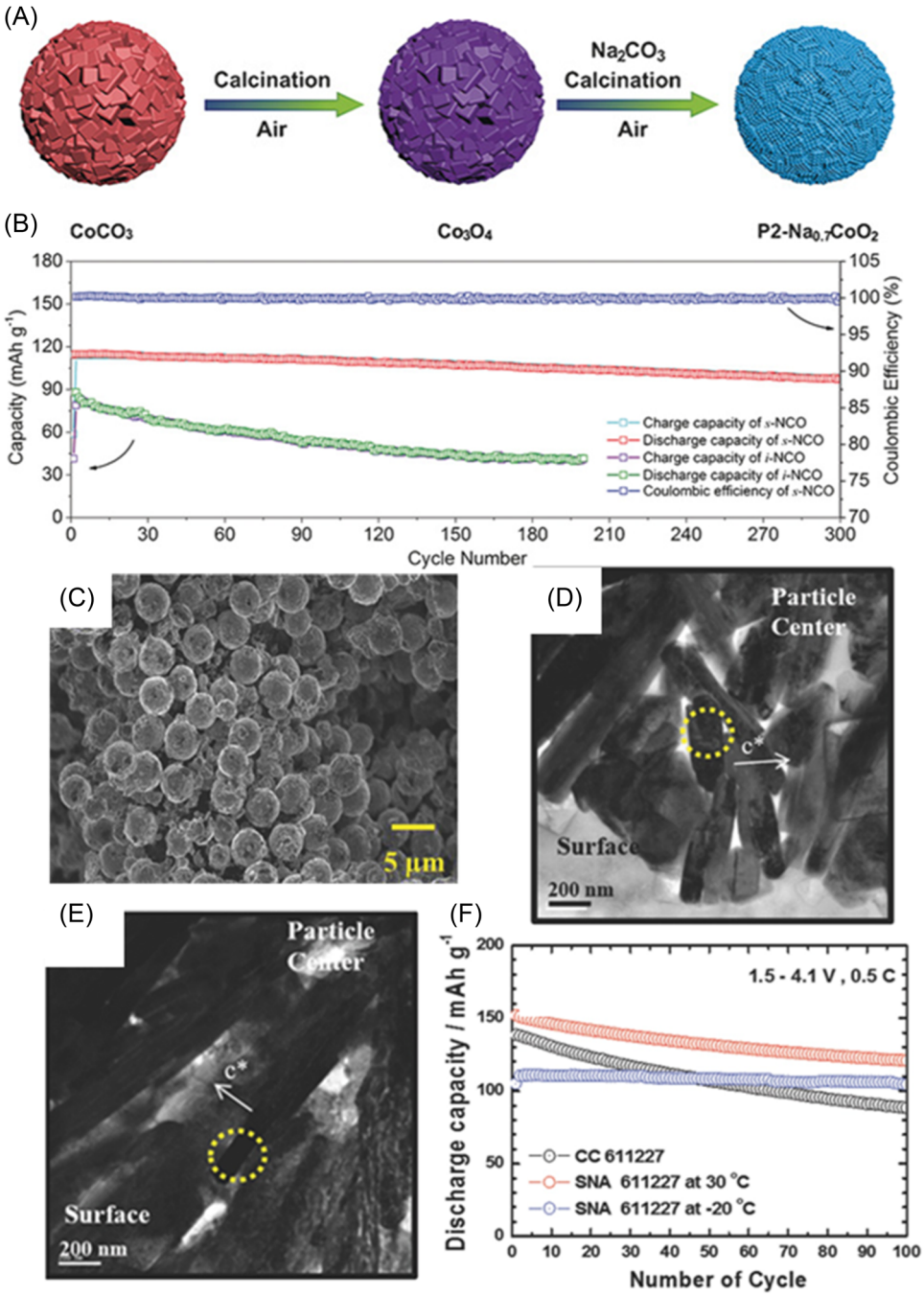

FIGURE 6 (A) Schematic illustration of the two-step synthesis of P2–$Na_{0.7}CoO_2$ microspheres. (B) Cycling performance of s–NCO and i–NCO at a current rate of 0.4 C and the corresponding Coulombic efficiency. Reproduced with permission: Copyright 2017, WILEY-VCH.[108] (C) Scanning electron microscope (SEM) images of Na–NMC-180. Reproduced with permission: Copyright 2018, WILEY-VCH.[109] (D) Bright-field transmission electron microscopy (TEM) images of CC $Na[Ni_{0.61}Co_{0.12}Mn_{0.27}]O_2$ particle. (E) Bright-field TEM images of spoke-like nanorods (SNA) $Na[Ni_{0.61}Co_{0.12}Mn_{0.27}]O_2$ particle. (F) Capacity retention of SNA during 100 cycles at 0.5 C rate. Reproduced with permission: Copyright 2016, WILEY-VCH.[110]

180°C by this method demonstrates high tap density up to 2.34 g/cm^3 and shows eminent cyclic stability (90% after 150 cycles) at a high cut-off voltage (4.7 V) (Figure 6C).[109] Moreover, if the spherical structure is composed of a hierarchical columnar structure, it may achieve interesting properties rather than reduced contact area and high tap density. For instance, designing the structures with inner high Ni composition and outer high Mn composition helps to realize higher specific capacity and better thermal and cycle stability.[111] Hwang et al. reported a compact composition-graded spherical $Na[Ni_{0.61}Co_{0.12}Mn_{0.27}]O_2$ cathode composed of spoke-like

nanorods (SNAs), which reduced porosity and enhanced the mechanical robustness. Compared with the constant–concentration (CC) counterpart, the primary nanorod particles are longer and align in a single direction to get a more compact structure (Figure 6D,E).[110] Benefiting from the grade concentration and special structure, the SNA cathode indicates improved cycle stability even at low temperatures (Figure 6F).

4.2 | Nanoflake and nanofiber structures

It is well known that nanotechnology has been proven to be a useful strategy to boost the storage behaviors of LTMO cathodes on account of shortened Na^+ diffusion paths, increased active reaction sites, decreased resistance caused by enlarged contact area with electrolyte, and reinforced structure.[112–114] Among these reported nanostructures, nanoflake or nanosheet structure is helpful to promote the rate performance of cathode materials.[115] Xiao et al. reported a multiple-layer oriented stacking nanosheets cathode which exposed {010} active facets, prepared by a thermal polymerization reaction (Figure 7A).[116] The exposed active facets and special stacking structure ensure fast Na^+ transfer and boost rate capacity by virtue of multiple channels and curtate diffusion distances, respectively. Therefore, the as-synthesized O3-type $Na[Li_{0.05}Ni_{0.3}Mn_{0.5}Cu_{0.1}Mg_{0.05}]O_2$ (O3-NaLNMCM) suggests pre-eminent rate capacity even at a high rate density up to 50 C (Figure 7B) and excellent capacity retention (91.9%) when cycled at 5 C after 600 cycles. Another $Na_{2/3}Ni_{1/6}Mn_{2/3}Cu_{1/9}Mg_{1/18}O_2$ (NaNMCM) electrode with a similar morphology not only shows the above-mentioned enhanced storage behaviors but also realizes solid–solution reaction mechanism, as confirmed by the in situ XRD measurement (Figure 7C).[117] One-dimensional fibrous nanostructure is also a significant structure that can effectively suppress the self-aggregation of nanoparticles resulted by their high surface energy, maintain good electrode–electrolyte contact, and stable crystal structure. Meanwhile, electrospinning extensively used in electrode material preparation is a viable and credible technique to produce consecutive porous nanofibers, and this low-cost craft can be appropriate for mass manufacturing.[119,120] Liu and coworkers prepared the representative $Na_{2/3}Ni_{1/3}Mn_{2/3}O_2$ cathode with the hierarchical fibrous structure by this technique. The distinctive porous nanofibers with diameters ranging from 200 to 600 nm are composed of abundant primary nanoparticles, and it efficiently accelerates Na^+ transfer because the electrolyte is in direct contact with the inner structure (Figure 7D,E).[118] Moreover, the pulverization and aggregation of the electrode material are also suppressed so that it shows outstanding rate performance (73.4 mA h/g at 20 C) and prolonged structural stability.

4.3 | Superlattice and vacancy structures

Cation migration during repeated electrochemical cycles leads to the gliding of the TM layers and the collapse of the host structure. Then, the LTMO cathodes go through slow kinetics and fast capacity decay.[67,101] In other words, the arrangement of Na^+ and TM ions plays an important role in determining structural stability. TM/TM-ordered superstructures can supply a stable layer to tolerate long-term Na^+ migration and retard the adverse migration of TM ions, which are distinct from the other two breakable ordered superstructures containing mobilizable Na^+ ions (Na^+/TM, Na^+/vacancy).[121,122] Ma et al. found that the superlattice in $NaMn_{0.6}Al_{0.4}O_2$ (NMA) cathode formed by the ordered arrangement of MnO_6 and AlO_6 octahedrons greatly reinforces the crystal structure, mitigates the Jahn–Teller effect, and hinders the TM-ions migration, thus the NMA maintains its original structure after 100 cycles compared with the $NaMnO_2$ (NMO) electrode without superstructure (Figure 8A).[35] Anion redox at high voltage provides extra capacity to enhance the energy density. However, different from the $Na_2Mn_3O_7$ cathode with small-voltage hysteresis, the irreversible oxygen activity in LTMO cathodes is always accompanied by large voltage hysteresis and oxygen release, further leading to the deterioration of host structure and fast capacity decay.[10,11] The superlattice can not only activate the oxygen redox reaction to provide outstanding specific capacity up to 285.9 mA h/g but also effectively suppress these negative effects.[125,126] Liu and coworkers introduced $Mg@Mn_6$ superstructure into the $Na_{0.73}Li_{0.11}Mg_{0.12}Mn_{0.77}O_2$ (NLMMO-1/2) cathode to offer a pinning effect to stabilize the crystal structure and restrain the oxygen loss. As confirmed by the high-resolution transmission electron microscope (HR-TEM), the $Na_{0.73}Li_{0.23}Mn_{0.77}O_2$ (NLMO) counterpart without superstructure shows severe cracks and crystal distortion after 10 cycles, while the NLMMO-1/2 still shows the intact layered structure (Figure 8B,C).[123] Meanwhile, the introduction of vacancies also plays a similar role with superlattice on oxygen activity. More specifically, this special structure facilitates anionic reaction by inducing nonbonding O 2p orbitals while vacancy-containing TMO_6 octahedrons with asymmetry and flexibility characters enable improved cycle stability.[62,127,128] Yang's group verified the existence of vacancies via advanced scanning transmission electron microscopic (STEM) measurement and revealed that

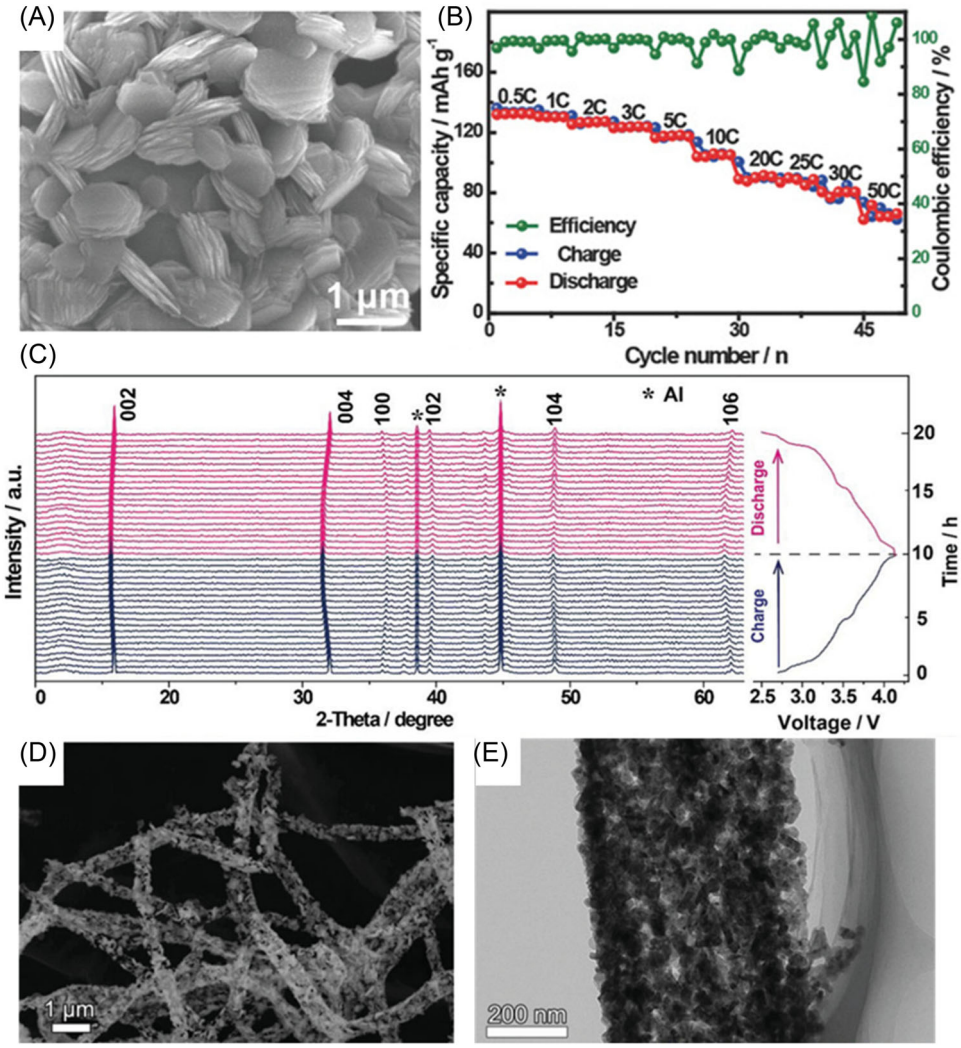

FIGURE 7 (A) Scanning electron microscope (SEM) image of O3–NaLNMCM material. (B) Rate performance of O3–NaLNMCM electrode at various rates. Reproduced with permission: Copyright 2018, WILEY-VCH.[116] (C) In situ X-ray diffraction (XRD) patterns of NaNMCM during the first cycle at 0.1 C in a voltage range of 2.5–4.15 V. Black asterisks represent peaks from the Al window. Reproduced with permission: Copyright 2019, WILEY-VCH.[117] (D) SEM images of $Na_{2/3}Ni_{1/3}Mn_{2/3}O_2$ nanofibers. (E) TEM images of $Na_{2/3}Ni_{1/3}Mn_{2/3}O_2$ nanofibers. Reproduced with permission: Copyright 2019, WILEY-VCH.[118]

vacancies in the as-prepared electrode can regulate the crystal structure to achieve better structural stability and reversible reaction.[129] In addition, Yuan et al. found that vacancies in $Na_{0.93}Li_{0.12}Ni_{0.25}Fe_{0.15}Mn_{0.48}O_2$ ($Na_{0.93}$ LNFM) also reduce the charge density of TM ions and boost the antioxidative capability. Thus this electrode shows less alkaline residue when exposed to air and ameliorated cycle stability (Figure 8D,E).[124]

5 | MIXED STRUCTURES

Though the hexagonal P2 phase provides direct diffusion pathways for Na^+ and hexagonal O3 possesses sufficient Na^+ in the host structure, it is still hard to obtain high specific capacity, eminent rate performance, and pre-eminent cycle stability simultaneously for single-phase structures due to their intrinsic drawbacks.[48,57] For instance, pure P2-type cathodes undergo deleterious P2–O2 or P2–OP4 phase transition at the deep desodiation state due to the gliding of TM layers, and it is even more complicated in a single O3 structure.[16] Designing a sample with mixed phases combines the merits of single phase and changes the spatial structure of pure phases. To date, many mixed structures, including P2/O3, P2/P3, layer-tunnel, and multiphases have been recorded to enhance the overall electrochemical performance, including superior energy efficiency and high Coulombic efficiency.[130–134]

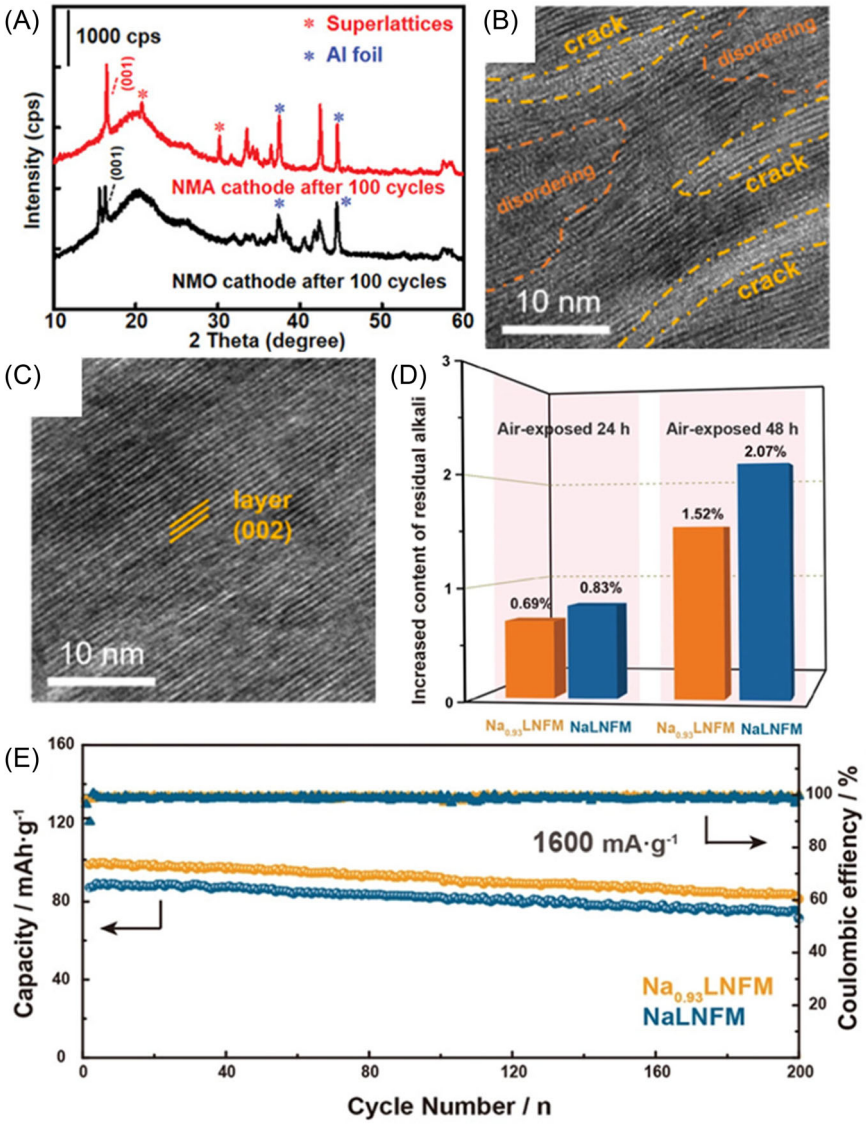

FIGURE 8 (A) X-ray diffraction (XRD) patterns of $NaMn_{0.6}Al_{0.4}O_2$ (NMA) and $NaMnO_2$ (NMO) cathodes after 100 cycles. Reproduced with permission: Copyright 2021, WILEY-VCH.[35] (B) High-resolution transmission electron microscopy (HRTEM) image of bulk structures for $Na_{0.73}Li_{0.23}Mn_{0.77}O_2$ (NLMO) after 10 cycles. (C) HRTEM image of bulk structures for NLMMO-1/2 after 10 cycles. Reproduced with permission: Copyright 2021, Elsevier Ltd.[123] (D) Chemical titration results before and after air exposure. (E) Cycling performance of $Na_{0.93}$LNFM and NaLNFM during 200 cycles at 1600 mA/g. Reproduced with permission: Copyright 2022, WILEY-VCH.[124]

5.1 | P2/O3 structures

P2/O3 composite structure is one of the most common mixed phases to solve the Na-deficient issue of P2 structure and the low-rate capacity and the complicated structure revolution of O3 structure, further facilitating the advance toward practical application. Moreover, this composite structure can be finely tuned to realize high reversible capacity and excellent cycle stability by meticulously modulating the composition of TM ions and the ratio between single phases.[135–137] Xiao et al. designed a new cathode material $Na_{2/3}Ni_{1/3}Mn_{1/3}Sn_{1/3}O_2$ with a P2/O3 bi-phase structure (P2/O3-NaNMS) by local chemistry modulation, which adjusts the formation energy and structural transformation to boost the intergrowth (Figure 9A).[138] Benefitting from the modulation strategy and synergistic effect of the heterostructure, the as-prepared composite electrode delivers enhanced rate performance (Figure 9B) accompanied by excellent long-cycle life when cycled at 2 C (capacity retention of 82.16% over 600 cycles). The boosted structural robustness was further verified by in situ XRD measurement. All the diffraction peaks return to their original position at the end of discharging, though they go through a reversible O3–P3 phase transition (Figure 9C). Encouraged by the good effects of composite structure, Chen's group reported another P2/O3 $Na_{0.67}Li_{0.11}Fe_{0.36}Mn_{0.36}Ti_{0.17}O_2$ (NLFMTO) electrode in which the structure was demonstrated by HR–TEM test (Figure 9D).[139] Compared with the P2-type Na–Fe–Mn oxide (NFMO), the biphasic structure effectively inhibits the P2–OP4 phase transition to mitigate the stress, thus achieving improved structural stability and prolonged cycle life (Figure 9E). In addition, as

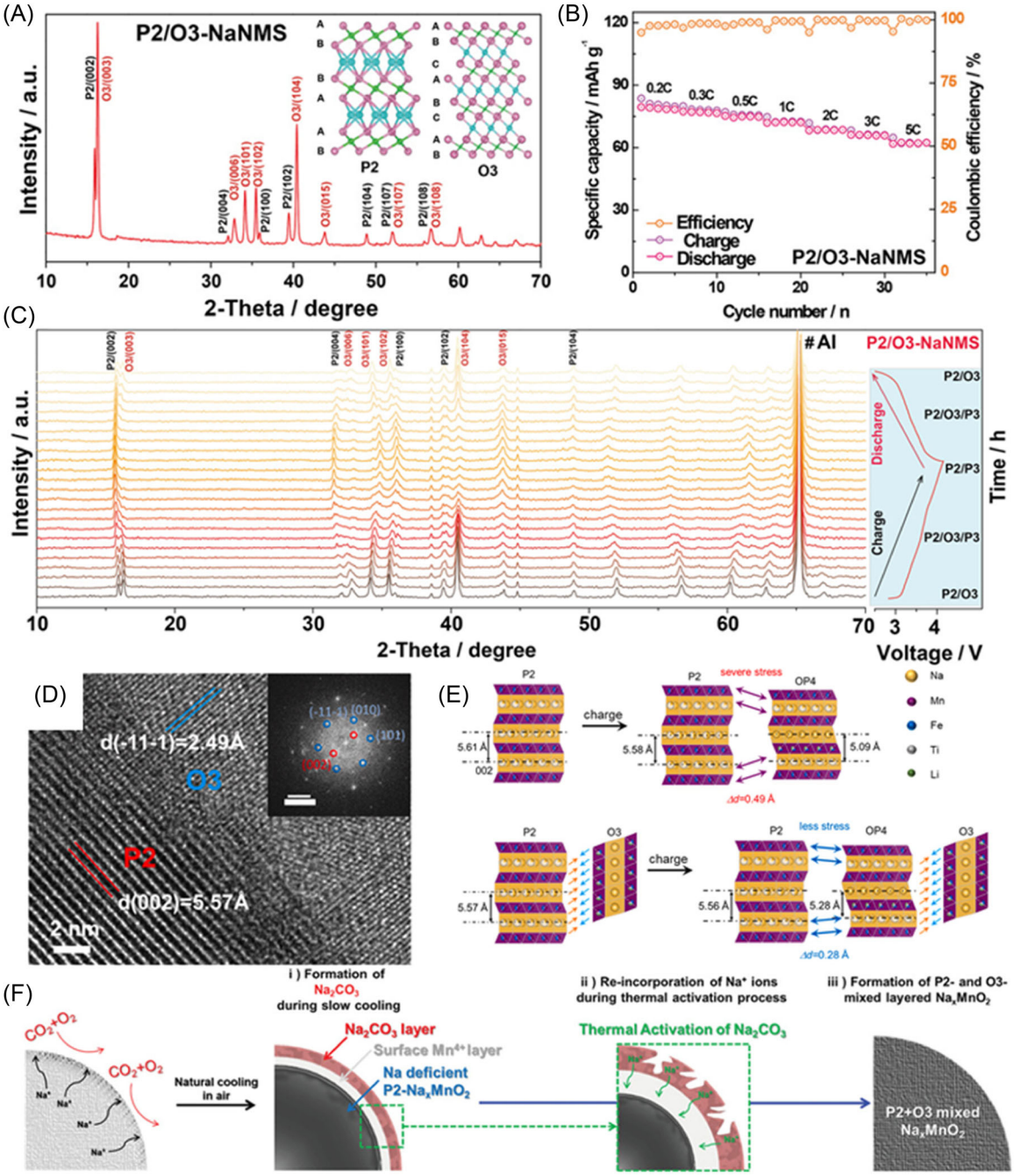

FIGURE 9 (A) Powder X-ray diffraction (XRD) pattern with P2-type and O3-type crystal structures. (B) Rate performance at various rates of P2/O3–NaNMS electrode. (C) In situ XRD patterns of P2/O3-NaNMS collected during the first charge/discharge at 0.1 C in the voltage range of 2.5–4.15 V. The black asterisks represent peaks from the Al window. Reproduced with permission: Copyright 2022, WILEY-VCH.[138] (D) High-resolution transmission electron microscopy (HRTEM) image at the phase boundary of NLFMTO. Inset is the corresponding FFT map. (E) Schematic view of the structure changes during the charge of Na–Fe–Mn oxide (NFMO) and $Na_{0.67}Li_{0.11}Fe_{0.36}Mn_{0.36}Ti_{0.17}O_2$ (NLFMTO). Reproduced with permission: Copyright 2021, Elsevier Ltd.[139] (F) Schematics for the formation of sodium carbonate on the surface of pristine NMO and thermal activation process to form activated $Na_{0.44}MnO_2$ (NMO) with P2 and O3 mixed framework. Reproduced with permission: Copyright 2021, WILEY-VCH.[140]

mentioned before, the LTMO cathodes easily react with air to produce insulated Na_2CO_3, leading to Na^+ loss and deteriorating the electronic and ionic conductivities.[45,46,140] Thermal activation of Na_2CO_3 on the surface of Na_xTMO_2 provides a possible way to solve this issue, which not only makes reuse of the active Na^+ but also generates mixed phase to promote the electrochemical properties (Figure 9F).[140]

5.2 | P2/P3 structures

In addition to the P2/O3 mixed-phase heterostructure, P2/P3 composite structure has also been extensively explored to pursue better performance because the P3-type cathode can deliver high specific capacity though it suffers from severe structural degradation. This kind of biphasic intergrowth can ignore the fragile crystal structure of the P3 phase resulting from low crystallinity and realize faster reaction kinetics and better cycle life compared with the single-phase component.[141–143] Zhou et al. reported a P2/P3–$Na_{0.7}Li_{0.06}Mg_{0.06}Ni_{0.22}Mn_{0.67}O_2$ (P2/P3–NLMNM) cathode material via a simple sol–gel reaction using citric and nitrates as raw materials, in which the structure was corroborated by XRD and HR-TEM tests (Figure 10A,B).[144] The synergistic effect ensures larger diffusion pathways and a stable structure to achieve enhanced specific capacity (119 mA h/g), rate performance (102 mA h/g at 5 C), and capacity retention (97.2% after 50 cycles) than single-phase counterparts.

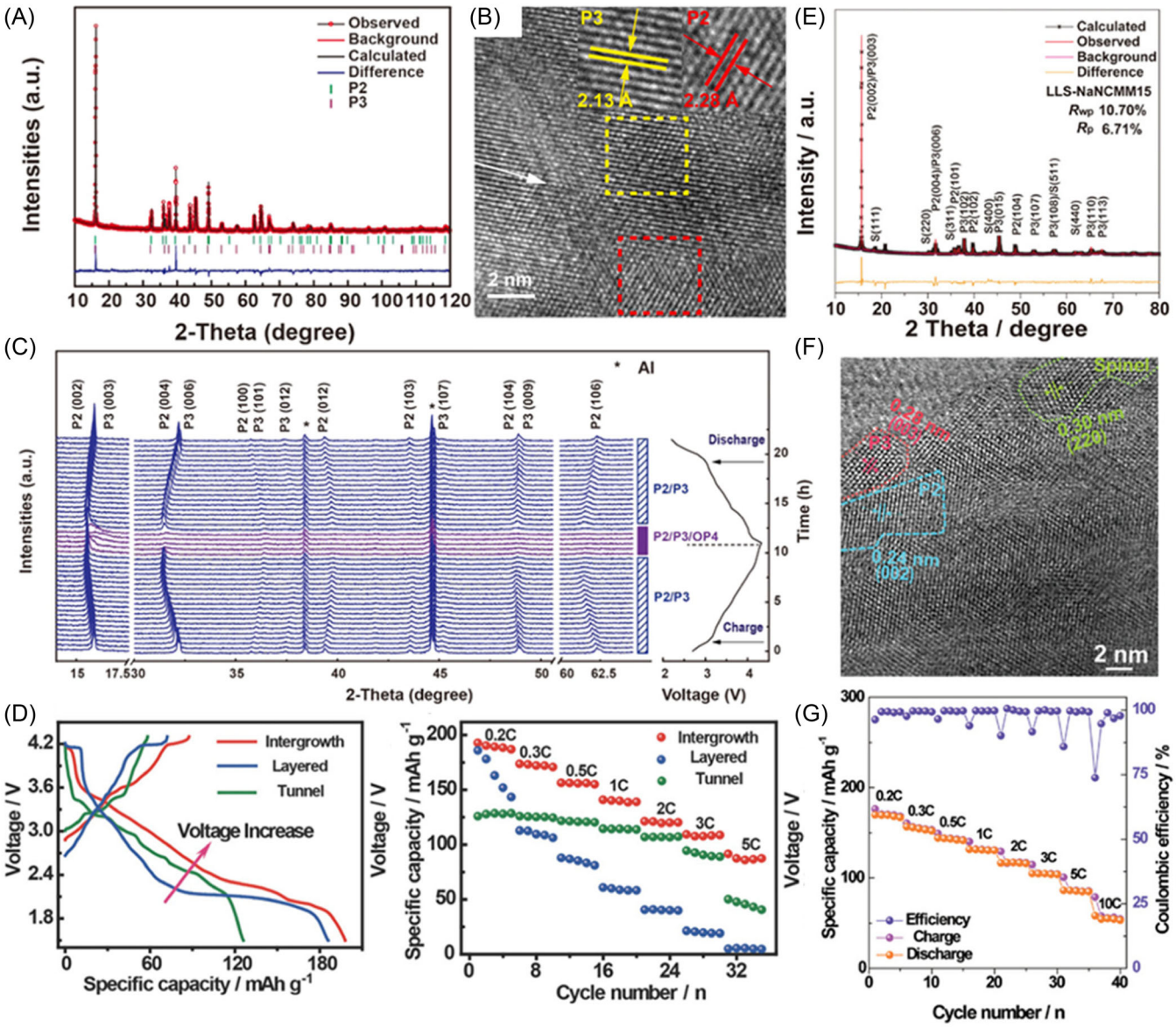

FIGURE 10 (A) Rietveld refinement patterns of the powder X-ray diffraction (XRD) data for P2/P3–NLMNM. (B) High-resolution transmission electron microscopy (HRTEM) image of P2/P3–NLNMM. (C) In situ XRD patterns of P2/P3–NLNMM collected during the 1st cycle of the cathode electrode under a 0.1 C rate. Reproduced with permission: Copyright 2018, Elsevier Ltd.[144] (D) First galvanostatic charge/discharge curves versus specific capacity and rate performance of layered, tunnel, and layered-tunnel intergrowth electrodes. Reproduced with permission: Copyright 2018, WILEY-VCH.[145] (E) Powder XRD pattern and Rietveld refinement plot of LLS–NaNCMM15 cathode. (F) HR–TEM image of P2 structure, P3 structure, and spinel structure. (G) Rate performance of LLS–NaNCMM15 electrode at various rates. Reproduced with permission: Copyright 2022, WILEY-VCH.[146]

Though reversible OP4/P3 phase transition is observed during the sodiation/desodiation process, it causes reduced stress than P2/P3–O2/P″3 direct phase transition by suppressing the gliding of TM layers to some extent, thereby boosting more stable structure (Figure 10C). Sometimes, the intergrowth structure can even display improvement in humidity resistance induced by element doping, providing a solution to solve one of the most serious issues for the commercial application of SIBs.[147]

5.3 | Layer-tunnel and multiphase structures

Though the insufficient Na^+ reserves in the host structure greatly limit its theoretical capacity, orthorhombic tunnel-type TM oxide cathode such as $Na_{0.44}MnO_2$ has garnered much attention on account of its distinct 3D structure and ample S tunnels, which are beneficial to achieve prolonged cycle stability and excellent rate performance. What is even more interesting is that the tunnel-type material is quite steady in water solution owing to its special structural frame composed of MnO_6 octahedra and MnO_5 square-pyramids, unlike the LTMO cathodes that are unstable when exposed to moisture. Hence, they can be applied to both aqueous and nonaqueous SIBs systems.[148,149] Intergrowth layer-tunnel structure optimizes the electrochemical performance by integrating the strengths of single phases. Thus the as-synthesized $Na_{0.6}MnO_2$ cathode with this composite structure synthesized by thermal polymerization reaction has a high specific capacity of 198.2 mA h/g and improved rate capacity (80.6 mA h/g at 5 C) compared to with the single-phase products (Figure 10D).[145] Moreover, the reversible mA h/g P2/tunnel–OP4/tunnel phase transition verified by in situ XRD test suggests its stable structure because the harmful P2–O2 structural revolution which causes large volume change and gliding of TM layers is effectively restrained. The layer–spinel composite structure also has been thoroughly studied, which shows superior properties because of the high electronic conductivity of the cubic spinel phase, though no detailed description is given here.[150,151] Except for these above-mentioned bi-phasic structures, in recent years, multiphase intergrowth heterostructures including P2/O3/O1, P3/P2/O3, P2/tunnel/O3′ (monoclinic structure), P2/P3/spinel, and so on have drawn much attention and opened a new field for promoting the development of LTMO cathodes. It is worth studying that the ratio of different structures can be tuned by adjusting the elemental stoichiometry to boost better electrochemical performance, such as superior energy efficiency and high Coulombic efficiency.[136,152–154]

Hu et al. reported a new $Na_{0.5}Ni_{0.05}Co_{0.15}Mn_{0.65}Mg_{0.15}O_2$ (LLS-NaNCMM15) cathode with P2/P3/spinel triphasic structure (Figure 10E,F) and introduced a strain engineering strategy which could triumphally tune the physical and chemical properties of this electrode material.[146] This technology, on the basis of local chemistry, greatly inhibits adverse structural revolution transition and contributes to low intrinsic stress. Thus the as-prepared material shows good structural stability though highly reversible P2/P3″/spinel phase transition is observed and displays superior rate performance (Figure 10G).

6 | SUMMARY AND OUTLOOK

Developing high-performance cathode materials for practical applications of SIBs is a significant measure for achieving a sustainable future. LTMO cathodes have been considered the most promising cathode materials owing to their high operating voltage, high specific capacity, and other merits. In this review, we comprehensively summarize the recent development status of LTMO cathodes for SIBs. In the meantime, several specific materials are listed in Table 1, including the compositions, modified methods, and electrochemical performance, to show the recent progress. Some severe issues that hindered the utilization potential of LTMO cathodes, such as low energy density, sluggish kinetics, structural rearrangement and revolution, and water/air sensitivity, are effectively handled by taking reasonable steps to optimize the performance (Scheme 1).

(1) Cationic ions can mitigate the gliding of the TM layers and inhibit the adverse phase transition at the deep desodiation process as well as restrain the Jahn–Teller effect of TM ions with low valence at the end of the discharging process. Anionic ion (F^-) greatly strengthens the chemical bonds, suppresses the dissolution of TM ions, and destroys the cation ordering. Doping facilitates diffusion kinetics, induces oxygen redox activity to deliver higher specific capacity, and promotes water/air stability to some extent. In addition, multielement substitution may bring about a synergistic effect and even contribute to forming a high entropy cathode, which further boosts the cycle stability.
(2) Surface coating with metal phosphate, metal oxide, metal fluoride, and so on can protect the active materials from direct contact with the electrolyte, effectively suppresses the side reactions, inhibits exfoliation of the active materials from the current collector, and mitigates HF attack. These protective layers can also mitigate the large volume change,

TABLE 1 A summary of current LTMO cathodes for SIBs focusing on compositions, modified methods, and electrochemical performance.

Material	Modified method	Voltage range (V)	Specific capacity (mA h/g)	Capacity retention
$Na_{0.67}[Mn_{0.61}Ni_{0.28}Sb_{0.11}]O_2$[52]	Sb doping	1.8–4.2	140 (0.1 C)	86% (200 cycles at 0.5 C)
$Na_{2/3}[(Ni_{0.5}Zn_{0.5})_{0.3}Mn_{0.7}]O_2$[55]	Zn doping	2.3–4.6	130 (26 mA/g)	95% (200 cycles at 26 mA/g)
$Na_{0.78}Ni_{0.31}Mn_{0.67}Nb_{0.02}O_2$[56]	Nb doping	2.4–4.15	96.6 (92 mA/g)	80% (500 cycles at 960 mA/g)
$Na_{0.67}Mn_{0.5}Co_{0.4}Fe_{0.1}O_2$[58]	Fe doping	1.5–4.0	/	71% (1000 cycles at 10 C)
$Na_{0.67}[Li_{0.21}Mn_{0.59}Ti_{0.2}]O_2$[60]	Ti doping	1.5–4.5	231 (0.2 C)	/
$[Na_{0.67}Zn_{0.05}]Ni_{0.18}Cu_{0.1}Mn_{0.67}$[63]	Zn/Cu doping	2.5–4.35	/	80.6% (2000 cycles at 10 C)
$Na_{0.7}Li_{0.03}Mg_{0.03}Ni_{0.27}Mn_{0.6}Ti_{0.07}O_2$[64]	Multidoping	2.2–4.4	116.8 (2 C)	82% (200 cycles at 2 C)
$NaNi_{0.25}Mg_{0.05}Cu_{0.1}Fe_{0.2}Mn_{0.2}Ti_{0.1}Sn_{0.1}O_2$[66]	Multidoping	2.0–4.0	130.8 (0.1 C)	75% (500 cycles at 1 C)
$Na_{2/3}Ni_{1/3}Mn_{2/3}O_{1.95}F_{0.05}$[71]	F doping	2.0–4.0	95.4 (2 C)	89% (400 cycles at 2 C)
$Na_{0.46}Mn_{0.93}Al_{0.07}O_{1.79}F_{0.21}$[72]	Al/F doping	1.8–4.0	164.3 (0.3 C)	89.1 (500 cycles at 5 C)
$Na_{0.7}MnO_{2.05}@NaPO_3$[80]	$NaPO_3$ coating	1.8–4.3	162 (0.1 A/g)	82% (200 cycles at 0.1 A/g)
$Na_{0.67}Ni_{0.28}Mg_{0.05}Mn_{0.67}O_2@NaTi_2(PO_4)_3$[83]	$NaTi_2(PO_4)_3$ coating	2.5–4.3	130.4 (0.1 C)	77.4% (200 cycles at 1 C)
Al_2O_3-$Na_{2/3}[Ni_{1/3}Mn_{2/3}]O_2$[87]	Al_2O_3 coating	2.5–4.3	160 (0.5 C)	73.2% (300 cycles at 0.5 C)
AlF-$Na[Ni_{0.65}Co_{0.08}Mn_{0.27}]O_2$[96]	AlF coating	1.5–4.1	168 (0.5 C)	90% (50 cycles at 0.5 C)
C-PDA-coated $Na_{0.80}Ni_{0.22}Zn_{0.06}Mn_{0.66}O_2$[98]	Carbon coating	2.0–4.3	124 (12 mA/g)	90.7% (100 cycles at 100 mA/g)
PI-coated $Na_{2/3}(Mn_{0.54}Ni_{0.13}Co_{0.13})O_2$[102]	Polyimide coating	2.0–4.5	133.16 (1 C)	70% (500 cycles at 5 C)
$Na_{0.66}(Ni_{0.13}Mn_{0.54}Co_{0.13})O_2$[109]	Microsphere	2.0–4.7	120 (1 C)	90% (150 cycles at 1 C)
$Na_{2/3}Ni_{1/6}Mn_{2/3}Cu_{1/9}Mg_{1/18}O_2$[117]	Nanoflake	2.5–4.15	87.9 (0.5 C)	81.4% (500 cycles at 5 C)
$Na_{2/3}Ni_{1/3}Mn_{2/3}O_2$[118]	Nanofiber	1.5–4.0	166.7 (0.1 C)	81% (500 cycles at 5 C)
$Na_{2/3}[Li_{1/7}Mn_{5/14}][Mg_{1/7}Mn_{5/14}]O_2$[125]	Superlattice	1.5–4.5	285.9 (0.1 C)	85.5% (50 cycles at 1 C)
$Na_{0.93}Li_{0.12}Ni_{0.25}Fe_{0.15}Mn_{0.48}O_2$[124]	Vacancy	2–4.2	130.1 (20 mA/g)	82.8% (200 cycles at 1600 mA/g)
$Na_{0.85}Ni_{0.34}Mn_{0.33}Ti_{0.33}O_2$[137]	P2/O3	2.2–4.4	126.6 (0.1 C)	80.6% (200 cycles at 1 C)
$Na_{0.78}Cu_{0.27}Zn_{0.06}Mn_{0.67}O_2$[147]	P2/P3	2.5–4.1	88 (0.1 C)	85% (200 cycles at 1 C)
$Na_{0.44}Co_{0.1}Mn_{0.9}O_2$[149]	Layer-tunnel	2.0–4.0	173.2 (0.2 C)	81.97% (100 cycles at 5 C)
$Na_{0.5}Ni_{0.1}Co_{0.15}Mn_{0.65}Mg_{0.1}O_2$[151]	P2/P3/spinel	1.5–4.0	153.8 (0.1 C)	80.6% (200 cycles at 2 C)

Abbreviations: LTMO, layered transition metal oxide; SIB, sodium-ion batteries.

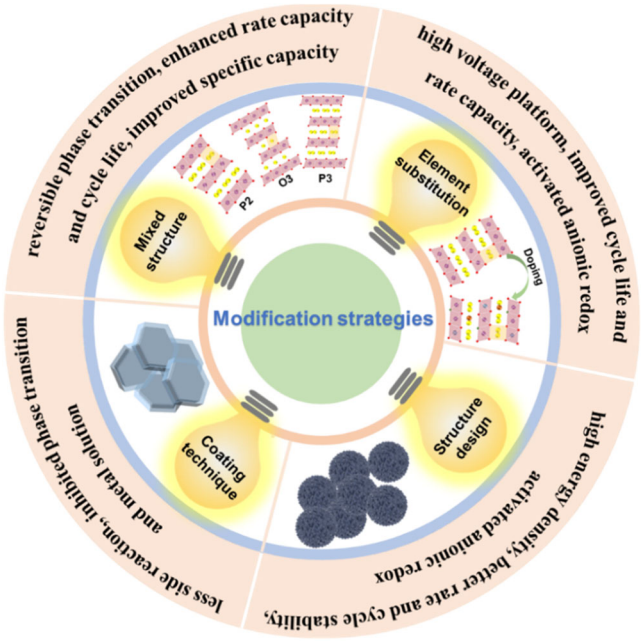

SCHEME 1 Summary of the merits of different modified strategies.

inhibit the harmful phase transition, retard metal dissolution, and buffer host structure against inherent strain and stress. Therefore, the structural stability and cycle life are improved. Meanwhile, TM ions with a larger radius in the coating material can dope into the crystal structure to increase the layer spacing, and materials with excellent conductivity can reduce the resistance, further promoting the rate performance.

(3) Reasonable morphology and structure design, including microsphere, nanoflake, and nanofiber, are useful to shorten the diffusion pathways for Na^+ and mitigate mechanical stress caused by Na^+ insertion/extraction. Moreover, the microspherical structure with high tap density is of great importance in increasing energy density. Superlattice and vacancy in the host structure not only stabilize the crystal structure but also activate the anionic redox to provide extra specific capacity. In the meantime, mixed structures (bi-phase/tri-phase) combining the merits of different single-phase components can achieve better cycle stability and rate performance, as well as reversible structural revolution.

These modified strategies actually do favor ameliorating the electrochemical performance because of the close structure–stoichiometry–properties relationship, leading to eminent rate capacity, cycling stability, higher specific capacity, and other improvements. However, existing LTMO cathodes face difficulty in meeting the requirements for practical applications and need to take measures to further optimize their performance. (1) Most of the doping elements are inactive, so partial substitution may cause a decrease in the specific capacity due to the reduced redox center. We need to explore lightweight element doping, such as boron, to minimize the sacrifice of specific capacity. (2) Surface coating and structure design are difficult to eliminate in the adverse phase transition intrinsically, so the improvement in cycle stability is limited, and it is necessary to integrate them with other modified methods to further promote the performance. (3) Mixed structures can greatly boost the electrochemical properties of LTMO cathodes because they successfully make good use of the merits of distinct structures, but how to precisely control the ratio of diverse structures is still a challenge. The proportion of each phase is closely related to the chemical stoichiometry and calcination temperature; thus, the ratios can be reasonably modulated by accurately adjusting these two parameters. (4) Low energy density caused by the relatively heavier and less-reducing potential of Na^+ is further hindered by cation-based charge compensation. Anionic redox reaction has been verified as an effective method to provide extra capacity at a high voltage range and realize high energy density of LTMO cathodes, greatly facilitating their potential for practical applications. Nevertheless, the anionic redox activated by forming some special configurations is accompanied by the release of oxygen, which can accelerate electrolyte degradation and migration of TM ions into the Na layers, further bringing about large volume stress, severe structure collapse, fast voltage decaying, irreversible structural revolution, and so on. It is difficult to realize superior capacity and excellent cycle life via a simple modified strategy in the LTMO cathodes with anionic redox activity. We need to get deep insight into the crystal structure change during the anionic redox and find a feasible solution to suppress oxygen release and TM-ion migration. The novel strain engineering strategy, on the basis of local chemistry, which tunes the physical and chemical properties, is a good selection to solve the above problems because it can effectively reduce lattice strain and restrain phase transformation. (5) Last but not least, the formation of an SEI layer on the surface of anode materials leads to irreversible Na^+ consumption in the first charging process while assembling sodium-ion full batteries, which could further impede the commercial application of Na-deficient P-type LTMO cathodes.[155,156] Sodium compensation, including anode presodiation, cathode sodium-rich, and cathode self-sacrificial additive methods, has been widely explored to solve this critical issue.[157,158] Although there are still some challenges that need to be solved to develop LTMO

cathodes with low cost, high specific capacity, high energy density, and superior cycle stability. Along this line, the utilization of LTMO cathodes in commercial SIB systems will be realized in the foreseeable future through the efforts of our researchers.

ACKNOWLEDGMENTS

J. X. and Y. X. contributed equally to this work. This project is financially supported by the Australian Research Council (ARC) through the ARC Discovery project (DP180102297) and Future Fellowship (FT180100705). J. X. is grateful for the financial support from China Scholarship Council. All authors thank the support from the Science and Technology Commission of Shanghai Municipality (No. 22010500400), "The Joint International Laboratory on Environmental and Energy Frontier Materials," and "Innovation Research Team of High–Level Local Universities in Shanghai" in Shanghai University.

CONFLICTS OF INTEREST STATEMENT

The authors declare no conflicts of interest.

ORCID

Hao Liu http://orcid.org/0000-0003-0266-9472

REFERENCES

1. Wang QC, Meng JK, Yue XY, et al. Tuning P2-structured cathode material by Na-site Mg substitution for Na-ion batteries. *J Am Chem Soc*. 2019;141(2):840-848.
2. Hwang JY, Kim J, Yu TY, Sun YK. A new P2-type layered oxide cathode with extremely high energy density for sodium-ion batteries. *Adv Energy Mater*. 2019;9(15):1803346.
3. Wang P-F, You Y, Yin Y-X, Guo Y-G. Layered oxide cathodes for sodium-ion batteries: phase transition, air stability, and performance. *Adv Energy Mater*. 2018;8(8):1701912.
4. Li L, Cao X, Huo J, et al. High valence metals engineering strategies of Fe/Co/Ni-based catalysts for boosted OER electrocatalysis. *J Energy Chem*. 2023;76:195-213.
5. Zhao C, Wang Q, Yao Z, et al. Rational design of layered oxide materials for sodium-ion batteries. *Science*. 2020;370(6517):708-711.
6. Kaliyappan K, Or T, Deng YP, Hu Y, Bai Z, Chen Z. Constructing safe and durable high-voltage P2 layered cathodes for sodium ion batteries enabled by molecular layer deposition of alucone. *Adv Funct Mater*. 2020;30(17):1910251.
7. Ding F, Meng Q, Yu P, et al. Additive-free self-presodiation strategy for high-performance Na-ion batteries. *Adv Funct Mater*. 2021;31(26):2101475.
8. Zhu H, Yao Z, Zhu H, et al. Unblocking oxygen charge compensation for stabilized high-voltage structure in P2-type sodium-ion cathode. *Adv Sci*. 2022;9(16):2200498.
9. Wang P-F, Xiao Y, Piao N, et al. Both cationic and anionic redox chemistry in a P2-type sodium layered oxide. *Nano Energy*. 2020;69:104474.
10. Abate I, Kim SY, Pemmaraju CD, et al. The role of metal substitution in tuning anion redox in sodium metal layered oxides revealed by X-ray spectroscopy and theory. *Angew Chem Int Ed*. 2021;60(19):10880-10887.
11. Kim EJ, Mofredj K, Pickup DM, Chadwick AV, Irvine JTS, Armstrong AR. Activation of anion redox in P3 structure cobalt-doped sodium manganese oxide via introduction of transition metal vacancies. *J Power Sources*. 2021;481:229010.
12. Gao A, Zhang Q, Li X, et al. Topologically protected oxygen redox in a layered manganese oxide cathode for sustainable batteries. *Nat Sustain*. 2022;5(3):214-224.
13. Jin Y, Le PML, Gao P, et al. Low-solvation electrolytes for high-voltage sodium-ion batteries. *Nat Energy*. 2022;7(8):718-725.
14. Yu TY, Ryu HH, Han G, Sun YK. Understanding the capacity fading mechanisms of O3-type $Na[Ni_{0.5}Mn_{0.5}]O_2$ cathode for sodium-ion batteries. *Adv Energy Mater*. 2020;10(37):2001609.
15. Zhao C, Yao Z, Wang J, et al. Ti Substitution facilitating oxygen oxidation in $Na_{2/3}Mg_{1/3}Ti_{1/6}Mn_{1/2}O_2$ cathode. *Chem*. 2019;5(11):2913-2925.
16. Song T, Chen L, Gastol D, et al. High-voltage stabilization of O3-type layered oxide for sodium-ion batteries by simultaneous tin dual modification. *Chem Mater*. 2022;34(9):4153-4165.
17. Fu H, Wang YP, Fan G, et al. Synergetic stability enhancement with magnesium and calcium ion substitution for Ni/Mn-based P2-type sodium-ion battery cathodes. *Chem Sci*. 2022;13(3):726-736.
18. Zhao S, Guo Z, Yang J, Wang C, Sun B, Wang G. Nanoengineering of advanced carbon materials for sodium-ion batteries. *Small*. 2021;17(48):2007431.
19. Rong X, Hu E, Lu Y, et al. Anionic redox reaction-induced high-capacity and low-strain cathode with suppressed phase transition. *Joule*. 2019;3(2):503-517.
20. Xiao J, Zhang F, Tang K, et al. Rational design of a P2-type spherical layered oxide cathode for high-performance sodium-ion batteries. *ACS Cent Sci*. 2019;5(12):1937-1945.
21. Lv WJ, Huang Z, Yin YX, Yao HR, Zhu HL, Guo YG. Strategies to build high-rate cathode materials for Na-ion batteries. *ChemNanoMat*. 2019;5(10):1253-1262.
22. Zuo W, Ren F, Li Q, et al. Insights of the anionic redox in P2-$Na_{0.67}Ni_{0.33}Mn_{0.67}O_2$. *Nano Energy*. 2020;78:105285.
23. Dong Y, Xu J, Chen M, et al. Self-assembled NaV_6O_{15} flower-like microstructures for high-capacity and long-life sodium-ion battery cathode. *Nano Energy*. 2020;68:104357.
24. Huang X, Li D, Huang H, Jiang X, Yang Z, Zhang W. Fast and highly reversible Na^+ intercalation/extraction in Zn/Mg dual-doped P2-$Na_{0.67}MnO_2$ cathode material for high-performance Na-ion batteries. *Nano Res*. 2021;14(10):3531-3537.
25. Cao X, Li X, Qiao Y, et al. Restraining oxygen loss and suppressing structural distortion in a newly Ti-substituted layered oxide P2-$Na_{0.66}Li_{0.22}Ti_{0.15}Mn_{0.63}O_2$. *ACS Energy Lett*. 2019;4(10):2409-2417.
26. Guo YJ, Wang PF, Niu YB, et al. Boron-doped sodium layered oxide for reversible oxygen redox reaction in Na-ion battery cathodes. *Nat Commun*. 2021;12(1):5267.
27. Ma X, Chen H, Ceder G. Electrochemical properties of monoclinic $NaMnO_2$. *J Electrochem Soc*. 2011;158(12):A1307-A1312.

28. Xiao J, Li X, Tang K, et al. Recent progress of emerging cathode materials for sodium-ion batteries. *Mater Chem Front*. 2021;5(10):3735-3764.
29. Li X, Shang Y, Yan D, Guo L, Huang S, Yang HY. Topotactic epitaxy self-assembly of potassium manganese hexacyanoferrate superstructures for highly reversible sodium-ion batteries. *ACS Nano*. 2022;16(1):453-461.
30. Tang Y, Li W, Feng P, et al. High-Performance manganese hexacyanoferrate with cubic structure as superior cathode material for sodium-ion batteries. *Adv Funct Mater*. 2020;30(10):1908754.
31. Zhou Y, Shao X, Lam K, et al. Symmetric sodium-ion battery based on dual-electron reactions of NASICON-structured $Na_3MnTi(PO_4)_3$ material. *ACS Appl Mater Interfaces*. 2020;12(27):30328-30335.
32. Zhang J, Liu Y, Zhao X, et al. A novel NASICON-type $Na_4MnCr(PO_4)_3$ demonstrating the energy density record of phosphate cathodes for sodium-ion batteries. *Adv Mater*. 2020;32(11):1906348.
33. Huangfu C, Liu Z, Lu X, Liu Q, Wei T, Fan Z. Strong oxidation induced quinone-rich dopamine polymerization onto porous carbons as ultrahigh-capacity organic cathode for sodium-ion batteries. *Energy Storage Mater*. 2021;43:120-129.
34. Shi Y, Li S, Gao A, et al. Probing the structural transition kinetics and charge compensation of the P2-$Na_{0.78}Al_{0.05}Ni_{0.33}Mn_{0.60}O_2$ cathode for sodium-ion batteries. *ACS Appl Mater Interfaces*. 2019;11(27):24122-24131.
35. Ma Z, Zhao Z, Xu H, et al. A queue-ordered layered Mn-based oxides with Al substitution as high-rate and high-stabilized cathode for sodium-ion batteries. *Small*. 2021;17(6):2006259.
36. Zhang L, Wang J, Schuck G, et al. Stabilizing P3-type oxides as cathodes for high-rate and long-life sodium ion batteries by disordered distribution of transition metals. *Small Methods*. 2020;4(10):2000422.
37. Wang Y, Zhao X, Jin J, et al. Low-cost layered oxide cathode involving cationic and anionic redox with a complete solid-solution sodium-storage behavior. *Energy Storage Mater*. 2022;47:44-50.
38. Zhang T, Ji H, Hou X, et al. Promoting the performances of P2-type sodium layered cathode by inducing Na site rearrangement. *Nano Energy*. 2022;100:107482.
39. Vanaphuti P, Yao Z, Liu Y, et al. Achieving high stability and performance in P2-type Mn-based layered oxides with tetravalent cations for sodium-ion batteries. *Small*. 2022;18(19):2201086.
40. Cheng C, Ding M, Yan T, et al. Anionic redox activities boosted by aluminum doping in layered sodium-ion battery electrode. *Small Methods*. 2022;6(3):2101524.
41. Huang Q, Wang M, Zhang L, et al. Shear-resistant interface of layered oxide cathodes for sodium ion batteries. *Energy Storage Mater*. 2022;45:389-398.
42. Yang L, Luo S, Wang Y, et al. Cu-doped layered P2-type $Na_{0.67}Ni_{0.33-x}Cu_xMn_{0.67}O_2$ cathode electrode material with enhanced electrochemical performance for sodium-ion batteries. *Chem Eng J*. 2021;404:126578.
43. Lamb J, Jarvis K, Manthiram A. Molten-salt synthesis of O3-type layered oxide single crystal cathodes with controlled morphology towards long-life sodium-ion batteries. *Small*. 2022;18(43):2106927.
44. Feng X, Li Y, Shi Q, et al. A comprehensive modification enables the high rate capability of P2-$Na_{0.75}Mn_{0.67}Ni_{0.33}O_2$ for sodium-ion cathode materials. *J Energy Chem*. 2022;69:442-449.
45. Wang J, Liu H, Yang Q, et al. Cu-doped P2-$Na_{0.7}Mn_{0.9}Cu_{0.1}O_2$ sodium-ion battery cathode with enhanced electrochemical performance: insight from water sensitivity and surface Mn(II) formation studies. *ACS Appl Mater Interfaces*. 2020;12(31):34848-34857.
46. Zuo W, Qiu J, Liu X, et al. The stability of P2-layered sodium transition metal oxides in ambient atmospheres. *Nat Commun*. 2020;11(1):3544.
47. Xiao J, Gao H, Tang K, et al. Manipulating stable layered P2-type cathode via a co-substitution strategy for high-performance sodium-ion batteries. *Small Methods*. 2022;6(3):2101292.
48. Ma C, Alvarado J, Xu J, et al. Exploring oxygen activity in the high energy P2-type $Na_{0.78}Ni_{0.23}Mn_{0.69}O_2$ cathode material for Na-ion batteries. *J Am Chem Soc*. 2017;139(13):4835-4845.
49. Shi Y, Zhang Z, Jiang P, et al. Unlocking the potential of P3 structure for practical sodium-ion batteries by fabricating zero strain framework for Na^+ intercalation. *Energy Storage Mater*. 2021;37:354-362.
50. Yang L, Li X, Liu J, et al. Lithium-doping stabilized high-performance P2-$Na_{0.66}Li_{0.18}Fe_{0.12}Mn_{0.7}O_2$ cathode for sodium-ion batteries. *J Am Chem Soc*. 2019;141(16):6680-6689.
51. Wang Y, Wang L, Zhu H, et al. Ultralow-strain Zn-substituted layered oxide cathode with suppressed P2-O2 transition for stable sodium ion storage. *Adv Funct Mater*. 2020;30(13):1910327.
52. Wang QC, Shadike Z, Li XL, et al. Tuning sodium occupancy sites in P2-layered cathode material for enhancing electrochemical performance. *Adv Energy Mater*. 2021;11(13):2003455.
53. Xiao B, Liu X, Chen X, et al. Uncommon behavior of Li doping suppresses oxygen redox in P2-type manganese-rich sodium cathodes. *Adv Mater*. 2021;33(52):2107141.
54. Cao X, Li H, Qiao Y, et al. Stabilizing reversible oxygen redox chemistry in layered oxides for sodium-ion batteries. *Adv Energy Mater*. 2020;10(15):1903785.
55. Konarov A, Kim HJ, Jo JH, et al. High-voltage oxygen-redox-based cathode for rechargeable sodium-ion batteries. *Adv Energy Mater*. 2020;10(24):2001111.
56. Shi Q, Qi R, Feng X, et al. Niobium-doped layered cathode material for high-power and low-temperature sodium-ion batteries. *Nat Commun*. 2022;13(1):3205.
57. Yang J, Tang M, Liu H, et al. O3-type layered Ni-rich oxide: a high-capacity and superior-rate cathode for sodium-ion batteries. *Small*. 2019;15(52):1905311.
58. Chu S, Zhang C, Xu H, Guo S, Wang P, Zhou H. Pinning effect enhanced structural stability toward a zero-strain layered cathode for sodium-ion batteries. *Angew Chem Int Ed*. 2021;60(24):13366-13371.
59. Jin T, Wang PF, Wang QC, et al. Realizing complete solid-solution reaction in high sodium content P2-type cathode for

high-performance sodium-ion batteries. *Angew Chem Int Ed*. 2020;59(34):14511-14516.
60. Xu H, Cheng C, Chu S, et al. Anion-cation synergetic contribution to high capacity, structurally stable cathode materials for sodium-ion batteries. *Adv Funct Mater*. 2020;30(50):2005164.
61. Zhou P, Che Z, Ma F, et al. Designing water/air-stable P2-layered cathodes with delayed P2-O2 phase transition by composition and structure engineering for sodium-ion batteries at high voltage. *Chem Eng J*. 2021;420:127667.
62. Shen Q, Liu Y, Zhao X, et al. Transition-metal vacancy manufacturing and sodium-site doping enable a high-performance layered oxide cathode through cationic and anionic redox chemistry. *Adv Funct Mater*. 2021;31(51):2106923.
63. Peng B, Chen Y, Wang F, et al. Unusual site-selective doping in layered cathode strengthens electrostatic cohesion of alkali-metal layer for practicable sodium-ion full cell. *Adv Mater*. 2022;34(6):2103210.
64. Cheng Z, Zhao B, Guo YJ, et al. Mitigating the large-volume phase transition of P2-type cathodes by synergetic effect of multiple ions for improved sodium-ion batteries. *Adv Energy Mater*. 2022;12(14):2103461.
65. Yao L, Zou P, Wang C, et al. High-entropy and superstructure-stabilized layered oxide cathodes for sodium-ion batteries. *Adv Energy Mater*. 2022;12(41):2201989.
66. Ding F, Zhao C, Xiao D, et al. Using high-entropy configuration strategy to design na-ion layered oxide cathodes with superior electrochemical performance and thermal stability. *J Am Chem Soc*. 2022;144(18):8286-8295.
67. Wang Q-C, Qiu Q-Q, Xiao N, et al. Tunnel-structured $Na_{0.66}[Mn_{0.66}Ti_{0.34}]O_{2-x}F_x$ (x<0.1) cathode for high-performance sodium-ion batteries. *Energy Storage Mater*. 2018;15:1-7.
68. Zhou C, Yang L, Zhou C, et al. Fluorine-substituted O3-type $NaNi_{0.4}Mn_{0.25}Ti_{0.3}Co_{0.05}O_2$−F cathode with improved rate capability and cyclic stability for sodium-ion storage at high voltage. *J Energy Chem*. 2021;60:341-350.
69. Hu H, He H-C, Xie R-K, et al. Achieving reversible Mn^{2+}/Mn^{4+} double redox couple through anionic substitution in a P2-type layered oxide cathode. *Nano Energy*. 2022;99:107390.
70. Kang W, Ma P, Liu Z, et al. Tunable electrochemical activity of P2-$Na_{0.6}Mn_{0.7}Ni_{0.3}O_{2-x}F_x$ microspheres as high-rate cathodes for high-performance sodium-ion batteries. *ACS Appl Mater Interfaces*. 2021;13(13):15333-15343.
71. Liu K, Tan S, Moon J, et al. Insights into the enhanced cycle and rate performances of the F-substituted P2-type oxide cathodes for sodium-ion batteries. *Adv Energy Mater*. 2020;10(19):2000135.
72. Chae MS, Kim HJ, Lyoo J, et al. Anomalous sodium storage behavior in Al/F dual-doped P2-type sodium manganese oxide cathode for sodium-ion batteries. *Adv Energy Mater*. 2020;10(43):2002205.
73. Cui X, Wang S, Ye X, et al. Insights into the improved cycle and rate performance by ex-situ F and in-situ Mg dual doping of layered oxide cathodes for sodium-ion batteries. *Energy Storage Mater*. 2022;45:1153-1164.
74. You Y, Song B, Jarvis K, Huq A, Manthiram A. Insights into the improved chemical stability against water of LiF-incorporated layered oxide cathodes for sodium-ion batteries. *ACS Mater Lett*. 2019;1(1):89-95.
75. Liu Z, Zhou C, Liu J, Yang L, Liu J, Zhu M. Phase tuning of P2/O3-type layered oxide cathode for sodium-ion batteries via a simple Li/F co-doping route. *Chem Eng J*. 2022;431:134273.
76. Zhang Y, Pei Y, Liu W, et al. $AlPO_4$-coated P2-type hexagonal $Na_{0.7}MnO_{2.05}$ as high stability cathode for sodium-ion battery. *Chem Eng J*. 2020;382:122697.
77. Zhang Y, Wu M, Ma J, et al. Revisiting the $Na_{2/3}Ni_{1/3}Mn_{2/3}O_2$ cathode: oxygen redox chemistry and oxygen release suppression. *ACS Cent Sci*. 2020;6(2):232-240.
78. Wang Y, Tang K, Li X, et al. Improved cycle and air stability of P3-$Na_{0.65}Mn_{0.75}Ni_{0.25}O_2$ electrode for sodium-ion batteries coated with metal phosphates. *Chem Eng J*. 2019;372:1066-1076.
79. Hwang J-Y, Yu T-Y, Sun Y-K. Simultaneous MgO coating and Mg doping of $Na[Ni_{0.5}Mn_{0.5}]O_2$ cathode: facile and customizable approach to high-voltage sodium-ion batteries. *J Mater Chem A*. 2018;6(35):16854-16862.
80. Li W, Yao ZJ, Zhang SZ, et al. Building superior layered oxide cathode via rational surface engineering for both liquid & solid-state sodium ion batteries. *Chem Eng J*. 2021;421:127788.
81. Jo C-H, Jo J-H, Yashiro H, Kim S-J, Sun Y-K, Myung S-T. Bioinspired surface layer for the cathode material of high-energy-density sodium-ion batteries. *Adv Energy Mater*. 2018;8(13):1702942.
82. Jo JH, Choi JU, Konarov A, et al. Sodium-ion batteries: building effective layered cathode materials with long-term cycling by modifying the surface via sodium phosphate. *Adv Funct Mater*. 2018;28(14):1705968.
83. Tang K, Huang Y, Xie X, et al. The effects of dual modification on structure and performance of P2-type layered oxide cathode for sodium-ion batteries. *Chem Eng J*. 2020;384:123234.
84. Li H, Wang T, Wang X, et al. Sodium superionic conductor $NaTi_2(PO_4)_3$ surface layer modified P2-type $Na_{2/3}Ni_{1/3}Mn_{2/3}O_2$ as high-performance cathode for sodium-ion batteries. *J Power Sources*. 2021;494:229771.
85. Li Y, Shi Q, Yin X, et al. Construction nasicon-type $NaTi_2(PO_4)_3$ nanoshell on the surface of P2-type $Na_{0.67}Co_{0.2}Mn_{0.8}O_2$ cathode for superior room/low-temperature sodium storage. *Chem Eng J*. 2020;402:126181.
86. Deng Q, Zheng F, Zhong W, et al. Nanoscale surface modification of P2-type $Na_{0.65}[Mn_{0.70}Ni_{0.16}Co_{0.14}]O_2$ cathode material for high-performance sodium-ion batteries. *Chem Eng J*. 2021;404:126446.
87. Liu Y, Fang X, Zhang A, et al. Layered P2-$Na_{2/3}[Ni_{1/3}Mn_{2/3}]O_2$ as high-voltage cathode for sodium-ion batteries: the capacity decay mechanism and Al_2O_3 surface modification. *Nano Energy*. 2016;27:27-34.
88. Joshua JR, Lee YS, Maiyalagan T, Nallamuthu N, Yuvraj P, Sivakumar N. $Na_{0.4}(Mn_{0.33}Co_{0.33}Ni_{0.33})O_2$ surface grafted with SnO nanorods: a cathode materials for rechargeable sodium-ion batteries. *J Electroanal Chem*. 2020;856:113633.
89. Yang Y, Dang R, Wu K, et al. Semiconductor material ZnO-coated P2-type $Na_{2/3}Ni_{1/3}Mn_{2/3}O_2$ cathode materials for sodium-ion batteries with superior electrochemical performance. *J Phys Chem C*. 2019;124(3):1780-1787.

90. Kaliyappan K, Liu J, Xiao B, et al. Enhanced performance of P2-$Na_{0.66}(Mn_{0.54}Co_{0.13}Ni_{0.13})O_2$ cathode for sodium-ion batteries by ultrathin metal oxide coatings via atomic layer deposition. *Adv Funct Mater*. 2017;27(37):1701870.
91. Hwang J-Y, Myung S-T, Choi JU, Yoon CS, Yashiro H, Sun Y-K. Resolving the degradation pathways of the O3-type layered oxide cathode surface through the nano-scale aluminum oxide coating for high-energy-density sodium-ion batteries. *J Mater Chem A*. 2017;5(45):23671-23680.
92. Kong W, Wang H, Sun L, Su C, Liu X. Understanding the synergic roles of MgO coating on the cycling and rate performance of $Na_{0.67}Mn_{0.5}Fe_{0.5}O_2$ cathode. *Appl Surf Sci*. 2019;497:143814.
93. Yu Y, Kong W, Li Q, et al. Understanding the multiple effects of TiO_2 coating on $NaMn_{0.33}Fe_{0.33}Ni_{0.33}O_2$ cathode material for Na-ion batteries. *ACS Appl Energy Mater*. 2020;3(1):933-942.
94. Alvarado J, Ma C, Wang S, Nguyen K, Kodur M, Meng YS. Improvement of the cathode electrolyte interphase on P2-$Na_{2/3}Ni_{1/3}Mn_{2/3}O_2$ by atomic layer deposition. *ACS Appl Mater Interfaces*. 2017;9(31):26518-26530.
95. Ji H, Zhai J, Chen G, et al. Surface engineering suppresses the failure of biphasic sodium layered cathode for high performance sodium-ion batteries. *Adv Funct Mater*. 2021;32(12):2109319.
96. Sun HH, Hwang JY, Yoon CS, Heller A, Mullins CB. Capacity degradation mechanism and cycling stability enhancement of AlF_3-coated nanorod gradient $Na[Ni_{0.65}Co_{0.08}Mn_{0.27}]O_2$ cathode for sodium-ion batteries. *ACS Nano*. 2018;12(12):12912-12922.
97. Liu Y, Yang J, Guo B, et al. Enhanced electrochemical performance of $Na_{0.5}Ni_{0.25}Mn_{0.75}O_2$ micro-sheets at 3.8 V for Na-ion batteries with nanosized-thin AlF_3 coating. *Nanoscale*. 2018;10(26):12625-12630.
98. Xia J, Wu W, Fang K, Wu X. Enhancing the interfacial stability of P2-type cathodes by polydopamine-derived carbon coating for achieving performance improvement. *Carbon*. 2020;157:693-702.
99. Lu D, Yao Z, Zhong Y, et al. Polypyrrole-coated sodium manganate hollow microspheres as a superior cathode for sodium-ion batteries. *ACS Appl Mater Interfaces*. 2019;11(17):15630-15637.
100. Quyen NQ, Van Nguyen T, Thang HH, Thao PM, Van Nghia N. Carbon coated $NaLi_{0.2}Mn_{0.8}O_2$ as a superb cathode material for sodium-ion batteries. *J Alloys Compd*. 2021;866:158950.
101. Zhuang Y, Zhao J, Zhao Y, Zhu X, Xia H. Carbon-coated single crystal O3-$NaFeO_2$ nanoflakes prepared via topochemical reaction for sodium-ion batteries. *Sustain Mater Technol*. 2021;28:e00258.
102. Kaliyappan K, Li G, Yang L, Bai Z, Chen Z. An ion conductive polyimide encapsulation: New insight and significant performance enhancement of sodium-based P2 layered cathodes. *Energy Storage Mater*. 2019;22:168-178.
103. Lin J, Huang Q, Dai K, et al. Mitigating interfacial instability of high-voltage sodium layered oxide cathodes with coordinative polymeric structure. *J Power Sources*. 2022;552:232235.
104. Xu H, Yan Q, Yao W, Lee C-S, Tang Y. Mainstream optimization strategies for cathode materials of sodium-ion batteries. *Small Struct*. 2022;3(4):2100217.
105. Wang X, Yin X, Feng X, et al. Rational design of $Na_{0.67}Ni_{0.2}Co_{0.2}Mn_{0.6}O_2$ microsphere cathode material for stable and low-temperature sodium ion storage. *Chem Eng J*. 2022;428:130990.
106. Xiao Y, Abbasi NM, Zhu YF, et al. Layered oxide cathodes promoted by structure modulation technology for sodium-ion batteries. *Adv Funct Mater*. 2020;30(30):2001334.
107. Wu F, Zhao C, Chen S, et al. Multi-electron reaction materials for sodium-based batteries. *Mater Today*. 2018;21(9):960-973.
108. Fang Y, Yu XY, Lou XWD. A practical high-energy cathode for sodium-ion batteries based on uniform P2-$Na_{0.7}CoO_2$ microspheres. *Angew Chem Int Ed*. 2017;56(21):5801-5805.
109. Kaliyappan K, Xaio W, Sham T-K, Sun X. High tap density Co and Ni containing P2-$Na_{0.66}MnO_2$ buckyballs: a promising high voltage cathode for stable sodium-ion batteries. *Adv Funct Mater*. 2018;28(32):1801898.
110. Hwang J-Y, Myung S-T, Yoon CS, Kim S-S, Aurbach D, Sun Y-K. Novel cathode materials for Na-ion batteries composed of spoke-like nanorods of $Na[Ni_{0.61}Co_{0.12}Mn_{0.27}]O_2$ assembled in spherical secondary particles. *Adv Funct Mater*. 2016;26(44):8083-8093.
111. Hwang JY, Oh SM, Myung ST, Chung KY, Belharouak I, Sun YK. Radially aligned hierarchical columnar structure as a cathode material for high energy density sodium-ion batteries. *Nat Commun*. 2015;6:6865.
112. Gao L, Chen S, Zhang L, Yang X. Self-supported $Na_{0.7}CoO_2$ nanosheet arrays as cathodes for high-performance sodium-ion batteries. *J Power Sources*. 2018;396:379-385.
113. Liang L, Sun X, Denis DK, et al. Ultralong layered $NaCrO_2$ nanowires: a competitive wide-temperature-operating cathode for extraordinary high-rate sodium-ion batteries. *ACS Appl Mater Interfaces*. 2019;11(4):4037-4046.
114. Mao Q, Gao R, Li Q, et al. O3-type $NaNi_{0.5}Mn_{0.5}O_2$ hollow microbars with exposed {0 1 0} facets as high-performance cathode materials for sodium-ion batteries. *Chem Eng J*. 2020;382:122978.
115. Soundharrajan V, Sambandam B, Alfaruqi MH, et al. $Na_{2.3}Cu_{1.1}Mn_2O_{7-\delta}$ nanoflakes as enhanced cathode materials for high-energy sodium-ion batteries achieved by a rapid pyrosynthesis approach. *J Mater Chem A*. 2020;8(2):770-778.
116. Xiao Y, Wang PF, Yin YX, et al. Exposing {010} active facets by multiple-layer oriented stacking nanosheets for high-performance capacitive sodium-ion oxide cathode. *Adv Mater*. 2018;30(40):1803765.
117. Xiao Y, Zhu YF, Yao HR, et al. A stable layered oxide cathode material for high-performance sodium-ion battery. *Adv Energy Mater*. 2019;9(19):1803978.
118. Liu Y, Shen Q, Zhao X, et al. Hierarchical engineering of porous P2-$Na_{2/3}Ni_{1/3}Mn_{2/3}O_2$ nanofibers assembled by nanoparticles enables superior sodium-ion storage cathodes. *Adv Funct Mater*. 2019;30(6):1907837.
119. Shen Q, Zhao X, Liu Y, et al. Dual-strategy of cation-doping and nanoengineering enables fast and stable sodium-ion storage in a novel Fe/Mn-based layered oxide cathode. *Adv Sci*. 2020;7(21):2002199.
120. Kalluri S, Seng KH, Pang WK, et al. Electrospun P2-type $Na_{2/3}(Fe_{1/2}Mn_{1/2})O_2$ hierarchical nanofibers as cathode material for

sodium-ion batteries. *ACS Appl Mater Interfaces*. 2014;6(12):8953-8958.
121. Huang Y, Zhu Y, Nie A, et al. Enabling anionic redox stability of P2-$Na_{5/6}Li_{1/4}Mn_{3/4}O_2$ by Mg substitution. *Adv Mater*. 2022;34(9):2105404.
122. Li Q, Xu S, Guo S, et al. A superlattice-stabilized layered oxide cathode for sodium-ion batteries. *Adv Mater*. 2020;32(23):1907936.
123. Liu J, Qi R, Zuo C, et al. Inherent inhibition of oxygen loss by regulating superstructural motifs in anionic redox cathodes. *Nano Energy*. 2021;88:106252.
124. Yuan XG, Guo YJ, Gan L, et al. A universal strategy toward air-stable and high-rate O3 layered oxide cathodes for Na-ion batteries. *Adv Funct Mater*. 2022;32(17):2111466.
125. Wang Q, Liao Y, Jin X, et al. Dual honeycomb-superlattice enables double-high activity and reversibility of anion redox for sodium-ion battery layered cathodes. *Angew Chem Int Ed*. 2022;61(33):e202206625.
126. Kim EJ, Maughan PA, Bassey EN, et al. Importance of superstructure in stabilizing oxygen redox in P3-$Na_{0.67}Li_{0.2}Mn_{0.8}O_2$. *Adv Energy Mater*. 2022;12(3):2102325.
127. Li XL, Bao J, Shadike Z, et al. Stabilizing transition metal vacancy induced oxygen redox by Co^{2+}/Co^{3+} redox and sodium-site doping for layered cathode materials. *Angew Chem Int Ed*. 2021;60(40):22026-22034.
128. Xiao B, Wang Y, Tan S, et al. Vacancy-enabled O3 phase stabilization for manganese-rich layered sodium cathodes. *Angew Chem Int Ed*. 2021;60(15):8258-8267.
129. Yang L, Liu Z, Liu S, et al. Superiority of native vacancies in activating anionic redox in P2-type $Na_{2/3}[Mn_{7/9}Mg_{1/9}\square_{1/9}]O_2$. *Nano Energy*. 2020;78:105172.
130. Yang L, Amo JML, Shadike Z, et al. A Co- and Ni-free P2/O3 biphasic lithium stabilized layered oxide for sodium-ion batteries and its cycling behavior. *Adv Funct Mater*. 2020;30(42):2003364.
131. Guo S, Liu P, Yu H, et al. A layered P2- and O3-type composite as a high-energy cathode for rechargeable sodium-ion batteries. *Angew Chem Int Ed*. 2015;54(20):5894-5899.
132. Li R, Liu Y, Wang Z, Li J. A P2/O3 biphasic cathode material with highly reversibility synthesized by Sn-substitution for Na-ion batteries. *Electrochim Acta*. 2019;318:14-22.
133. Hu B, Geng F, Zhao C, et al. Deciphering the origin of high electrochemical performance in a novel Ti-substituted P2/O3 biphasic cathode for sodium-ion batteries. *ACS Appl Mater Interfaces*. 2020;12(37):41485-41494.
134. Li X, Xu J, Li H, Zhu H, Guo S, Zhou H. Synergetic anion-cation redox ensures a highly stable layered cathode for sodium-ion batteries. *Adv Sci*. 2022;9(16):2105280.
135. Liang X, Sun YK. A novel pentanary metal oxide cathode with P2/O3 biphasic structure for high-performance sodium-ion batteries. *Adv Funct Mater*. 2022;32(44):2206154.
136. Liang X, Yu T-Y, Ryu H-H, Sun Y-K. Hierarchical O3/P2 heterostructured cathode materials for advanced sodium-ion batteries. *Energy Storage Mater*. 2022;47:515-525.
137. Yu L, Cheng Z, Xu K, et al. Interlocking biphasic chemistry for high-voltage P2/O3 sodium layered oxide cathode. *Energy Storage Mater*. 2022;50:730-739.
138. Xiao Y, Wang HR, Hu HY, et al. Formulating high-rate and long-cycle heterostructured layered oxide cathodes by local chemistry and orbital hybridization modulation for sodium-ion batteries. *Adv Mater*. 2022;34(33):2202695.
139. Chen C, Huang W, Li Y, et al. P2/O3 biphasic Fe/Mn-based layered oxide cathode with ultrahigh capacity and great cyclability for sodium-ion batteries. *Nano Energy*. 2021;90:106504.
140. Yang J, Lim JM, Park M, et al. Thermally activated P2-O3 mixed layered cathodes toward synergistic electrochemical enhancement for Na ion batteries. *Adv Energy Mater*. 2021;11(44):2102444.
141. Xue L, Shi X, Lin B, Guo Q, Zhao Y, Xia H. Self-standing P2/P3 heterostructured $Na_{0.7}CoO_2$ nanosheet arrays as 3D cathodes for flexible sodium-ion batteries. *J Power Sources*. 2020;457:228059.
142. Jo JH, Kim HJ, Choi JU, et al. Facilitating sustainable oxygen-redox chemistry for P3-type cathode materials for sodium-ion batteries. *Energy Storage Mater*. 2022;46:329-343.
143. Paidi AK, Park WB, Ramakrishnan P, et al. Unravelling the nature of the intrinsic complex structure of binary-phase Na-layered oxides. *Adv Mater*. 2022;34(29):2202137.
144. Zhou Y-N, Wang P-F, Niu Y-B, et al. A P2/P3 composite layered cathode for high-performance Na-ion full batteries. *Nano Energy*. 2019;55:143-150.
145. Xiao Y, Wang P-F, Yin Y-X, et al. A layered-tunnel intergrowth structure for high-performance sodium-ion oxide cathode. *Adv Energy Mater*. 2018;8(22):1800492.
146. Hu HY, Zhu YF, Xiao Y, et al. Strain engineering by local chemistry manipulation of triphase heterostructured oxide cathodes to facilitate phase transitions for high-performance sodium-ion batteries. *Adv Energy Mater*. 2022;12(32):2201511.
147. Yan Z, Tang L, Huang Y, et al. A hydrostable cathode material based on the layered P2@P3 composite that shows redox behavior for copper in high-rate and long-cycling sodium-ion batteries. *Angew Chem Int Ed*. 2019;58(5):1412-1416.
148. Chae MS, Kim HJ, Bu H, et al. The sodium storage mechanism in tunnel-type $Na_{0.44}MnO_2$ cathodes and the way to ensure their durable operation. *Adv Energy Mater*. 2020;10(21):2000564.
149. Xiao Y, Zhu YF, Xiang W, et al. Deciphering an abnormal layered-tunnel heterostructure induced by chemical substitution for the sodium oxide cathode. *Angew Chem Int Ed*. 2020;59(4):1491-1495.
150. Vanam SP, Barpanda P. A molybdenum doped layer-spinel composite cathode material for sodium-ion battery. *Electrochim Acta*. 2022;431:141122.
151. Zhu YF, Xiao Y, Hua WB, et al. Manipulating layered P2@P3 integrated spinel structure evolution for high-performance sodium-ion batteries. *Angew Chem Int Ed*. 2020;59(24):9299-9304.
152. Cheng Z, Fan XY, Yu L, et al. A rational biphasic tailoring strategy enabling high-performance layered cathodes for

sodium-ion batteries. *Angew Chem Int Ed*. 2022;61(19): e202117728.
153. Jiang N, Liu Q, Wang J, et al. Tailoring P2/P3 biphases of layered Na_xMnO_2 by Co substitution for high-performance sodium-ion battery. *Small*. 2021;17(7):2007103.
154. Li R, Gao J, Li J, et al. An undoped tri-phase coexistent cathode material for sodium-ion batteries. *Adv Funct Mater*. 2022;32(41):2205661.
155. Sathiya M, Thomas J, Batuk D, Pimenta V, Gopalan R, Tarascon JM. Dual stabilization and sacrificial effect of Na_2CO_3 for increasing capacities of Na-ion cells based on P2-Na_xMO_2 electrodes. *Chem Mater*. 2017;29(14):5948-5956.
156. Pan X, Chojnacka A, Béguin F. Advantageous carbon deposition during the irreversible electrochemical oxidation of $Na_2C_4O_4$ used as a presodiation source for the anode of sodium-ion systems. *Energy Storage Mater*. 2021;40:22-30.
157. Niu YB, Guo YJ, Yin YX, et al. High-efficiency cathode sodium compensation for sodium-ion batteries. *Adv Mater*. 2020;32(33):2001419.
158. Liu X, Tan Y, Liu T, et al. A simple electrode-level chemical presodiation route by solution spraying to improve the energy density of sodium-ion batteries. *Adv Funct Mater*. 2019;29(50):1903795.

AUTHOR BIOGRAPHIES

Jun Xiao obtained his bachelor's degree in Chemical Engineering and Technology at Changzhou University in 2017. He is pursuing his PhD degree at Shanghai University. He is also currently a joint PhD candidate at the University of Technology Sydney, supported by the China Scholarship Council. His research interest mainly focuses on metal oxide cathode materials for sodium-ion batteries.

Yang Xiao obtained his bachelor's degree in Chemical Engineering and Technology at Hefei University of Technology in 2021. He is pursuing his master's degree at Shanghai University. His research interest mainly focuses on metal oxide cathode materials and Prussian blue cathode materials for sodium-ion batteries.

Jiayi Li obtained her master's degree in Physics at Qingdao University in 2021. She is pursuing her PhD degree at Shanghai University. Her research interest mainly focuses on cathodes materials for lithium sulfur and sodium selenium batteries.

Cheng Gong obtained his bachelor's degree in East China University of Technology in 2021. He is pursuing a master's degree at Shanghai University, and his research interest mainly focuses on metal oxide anode materials used in lithium-ion batteries.

Xinming Nie is a senior experimenter at the School of Physics and Electronic Engineering of Jiangsu Normal University. He received a bachelor's degree from Huaiyin Institute of Technology in Jiangsu Province, a master's degree from the Guangdong University of Technology, and a doctoral candidate from the China University of Mining and Technology. His research interests focus on high-safety and high-performance lithium-ion, zinc-ion batteries, and other high-energy-density batteries.

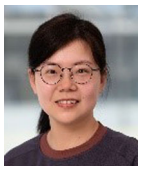

Hong Gao received her PhD in material science at University of Wollongong, Australia in 2018. Currently, she is working as a lecturer at School of Environmental and Chemical Engineering, Shanghai University. Her research interests focus on energy storage materials for lithium-, sodium- and potassium-ion batteries.

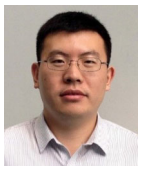

Bing Sun received his bachelor's degree (2005) and master's degree (2007) from Harbin Institute of Technology (HIT), China and completed his PhD in 2012 at University of Technology Sydney (UTS), Australia. Currently, he is a senior lecturer and Australia Research Council Future Fellow at UTS. His current research interests focus on the synthesis and characterization of functional materials and their applications in energy storage devices beyond lithium ion batteries, including lithium/sodium oxygen batteries, lithium/sodium sulfur batteries and potassium ion batteries.

Hao Liu obtained his PhD degree from the University of Wollongong in 2011. He worked as a research associate at the University of Queensland and moved to the University of Technology Sydney as a Chancellor's postdoctoral research fellow. He is a Future Fellow awarded by Australian Research

Council. Dr. Liu is interested in the synthesis of nanostructured materials and their applications in the fields of lithium-ion batteries, sodium-ion batteries, lithium–sulfur batteries, lithium–oxygen batteries, supercapacitors, and electrocatalysts.

Guoxiu Wang is a Distinguished Professor and the Director of the Centre for Clean Energy Technology at the University of Technology Sydney. He has been working in the areas of materials science and engineering, materials chemistry, electrochemistry, energy storage and conversion, battery technology, and nanoscience and nanotechnology for over 20 years. He has performed extensive research on electromaterials for applications in rechargeable lithium-ion batteries, lithium-air batteries, sodium-ion batteries, lithium–sulfur batteries, supercapacitors, electrocatalysts, and fuel cells, as well as controllable synthesis of one-dimensional semiconductor nanostructures and their applications for chemical and biosensors, and semiconductor quantum dots, quantum wires, and quantum tubes for nanoscale electronic and photonic devices.

How to cite this article: Xiao J, Xiao Y, Li J, et al. Advanced nanoengineering strategies endow high-performance layered transition-metal oxide cathodes for sodium-ion batteries. *SmartMat*. 2023;4:e1211. doi:10.1002/smm2.1211